Stochastic surrogate model for meteotsunami early warning system in the eastern Adriatic Sea

Cléa Denamiel[1]*, Jadranka Šepić[1], Xun Huan[2], Célia Bolzer[3,4], Ivica Vilibić[1]

[1] Institute of Oceanography and Fisheries, Šetalište I. Meštrovića 63, 21000 Split, Croatia
[2] University of Michigan, 2033 AL, 1231 Beal Ave, Ann Arbor, MI 48109-2133, U.S.A.
[3] SeaTech, Ecole d'ingénieurs - Université de Toulon, CS 60584, 83041 Toulon Cedex 9, France
[4] EniProgetti Eni House, Basing View, Basingstoke, Hampshire, RG21 4YY, U.K.

*Corresponding author: Cléa Denamiel (cdenamie@izor.hr)

Key Points

- Design and evaluation of an innovative meteotsunami early warning system prototype using stochastic surrogate approach
- Forecast of the atmospheric internal gravity waves driving meteotsunami events with deterministic state-of-the-art models
- Stochastic surrogate model based on generalized polynomial chaos expansion methods and running at nearly no computational cost

Abstract

The meteotsunami early warning system prototype using stochastic surrogate approach and running operationally in the eastern Adriatic Sea is presented. First, the atmospheric Internal Gravity Waves (IGWs) driving the meteotsunamis are either forecasted with state-of-the-art deterministic models at least a day in advance or detected through measurements at least 2-h before the meteotsunami reaches sensitive locations. The extreme sea-level hazard forecast at endangered locations is then derived with an innovative stochastic surrogate model – implemented with generalized Polynomial Chaos Expansion (gPCE) method and synthetic IGWs

This is the author manuscript accepted for publication and has undergone full peer review but has not been through the copyediting, typesetting, pagination and proofreading process, which may lead to differences between this version and the Version of Record. Please cite this article as doi: 10.1029/2019JC015574

Author Manuscript

This article is protected by copyright. All rights reserved.

forcing a barotropic ocean model – used with the input parameters extracted from deterministic model results and/or measurements. The evaluation of the system, both against five historical events and for all the detected potential meteotsunamis since late 2018 when the early warning system prototype became operational, reveals that the meteotsunami hazard is conservatively assessed but often overestimated at some locations. Despite some needed improvements and developments, this study demonstrates that gPCE-based methods can be used for atmospherically-driven extreme sea-level hazard assessment, and in geosciences in wide.

Plain Language Summary

Atmospherically-driven extreme sea-level events are one of the major threats to people and assets in the coastal regions. Assessing the hazard associated with such events together with uncertainty quantification in a precise and timely manner is thus of primary importance in modern societies. In this study, an early warning system for the eastern Adriatic meteotsunamis – destructive long waves with periods from few minutes up to an hour generated by traveling atmospheric disturbances, is presented and evaluated. The system is based on state-of-the-art deterministic atmospheric and ocean models as well as an innovative statistical model developed to forecast the meteotsunami hazard. The evaluation reveals that the meteotsunami hazard is conservatively assessed but often overestimated. This study demonstrates that the presented methodology can be used for extreme sea-level hazard assessment and in general for hazard studies in geosciences.

Key Words

Meteotsunami early warning system, extreme sea-level hazard assessment, eastern Adriatic

This article is protected by copyright. All rights reserved.

Author Manuscript

1 Introduction

During the past decade, meteorological tsunamis or meteotsunamis – destructive long waves in the tsunami frequency band generated by traveling atmospheric disturbances (Monserrat et al., 2006), have become the object of an increasing number of studies all over the globe (Tanaka, 2010; Šepić et al., 2012; Cho et al., 2013; Okal et al., 2014; Pattiaratchi & Wijeratne, 2014; Pellikka et al., 2014; Whitmore & White, 2014; Olabarrieta et al., 2017, Masina et al., 2017; Dusek et al., 2019). These extreme events have the potential to produce substantial damages to houses, goods and infrastructures (Hibiya & Kajiura, 1982; Salaree et al., 2018; Linares et al., 2019) – e.g. more than seven million US dollar losses in Vela Luka harbor, Croatia during the 21st of June 1978 meteotsunami (Vučetić et al., 2009; Orlić et al., 2010), but also to claim human lives – e.g. seven people killed during a sunny day in 1954 (Ewing et al., 1954) in the Great Lakes near Chicago, USA. Rather than addressing a particular catastrophic event, this work focuses on the design and evaluation of an innovative meteotsunami early warning system tested in operational mode, since late 2018, in the eastern Adriatic. As fully preventing meteotsunami impact is, for now, close to impossible (Vilibić et al., 2016), the principal goal of such a system is to allow the local communities to better prepare for these destructive events (e.g. set temporary protection against flooding and waves, avoid swimming, etc.) in order to minimize the losses. However, deterministically forecasting the atmospheric disturbances responsible for meteotsunamis is challenging (Renault et al., 2011; Denamiel et al., 2019) and the uncertainties in anticipating their location and intensity as well as their relationship to flood in sensitive harbor locations must be taken into account. In addition, as meteotsunamis are rare events which require specific model setup – e.g. for the ocean, a 1-min atmospheric forcing and a resolution below 50m in the harbors where resonance occurs, the available forecast

Author Manuscript

This article is protected by copyright. All rights reserved.

results are generally not designed to capture them (Denamiel et al., 2019). For the Adriatic Sea, a specific numerical suite was thus implemented to deterministically forecast the atmospheric disturbances – e.g. the Internal Gravity Waves (IGWs; Vilibić & Šepić, 2009; Denamiel et al., 2019), driving the meteotsunamis along the Croatian coastline.

In order to quantify the uncertainties linked to the meteotsunami extreme sea-levels, the origin, propagation and sources of uncertainty of the complex ocean-atmosphere system must be described (Arnst & Ponthot, 2014; Ghanem et al., 2017; Bulthuis et al., 2019). In the Adriatic Sea, the location, speed, period, amplitude and direction of the forecasted atmospheric disturbances are the primary sources of uncertainties linked to the meteotsunami events and can thus be seen as random variables characterized by their prior distributions. In the field of uncertainty quantification (Le Maître & Knio, 2010; Ghanem et al., 2017), generalized Polynomial Chaos Expansion (gPCE) methods (Xiu & Karniadakis, 2002; Soize & Ghanem, 2004) have been widely used to build surrogate models that propagate, at nearly no computational cost, the uncertainties of a given stochastic forcing to the results of a deterministic model. Furthermore, in the past decade, gPCE methods have been applied with success in geosciences: Formaggia et al. (2013) built a surrogate model of basin-scale geochemical compaction, Wang et al. (2016) studied the acoustic uncertainty predictions, Sraj et al. (2014) estimated the wind drag parameter forcing an ocean model, Giraldi et al. (2017) documented the propagation of earthquake ocean floor displacement uncertainty to the tsunami wave parameters and Bulthuis et al. (2019) used a surrogate model to quantify the uncertainty of the multi-centennial response of the Antarctic ice sheet to climate change. Following the footsteps of these recent studies, the newly developed meteotsunami surrogate model was thus designed to propagate the known uncertainties of the atmospheric disturbances to the forecast of extreme

This article is protected by copyright. All rights reserved.

sea-levels at five sensitive locations along the Croatian coastline: Vela Luka, Vrboska, Stari Grad, Rijeka dubrovačka and Ston (Fig. 1).

In this paper, the setup of the Croatian early warning system prototype, which provides meteotsunami hazard assessments depending on the deterministically forecasted and measured atmospheric pressure waves and the stochastically deduced maximum elevation distributions derived with the surrogate model, is first described in details in Section 2. In section 3, its evaluation for five different locations along the Croatian coastline is performed first, against five different historical events, and then for automatically detected events since the system became operational in late 2018. Finally, the methodological choices made to design this first meteotsunami early warning system as well as its performance and the improvements needed to increase its reliability are discussed in Section 4.

2 Design of the meteotsunami early warning system

2.1 Data and models

The Croatian Meteotsunami Early Warning System (CMeEWS, Šepić et al., 2017) – developed within the framework of the project MESSI ("Meteotsunamis, destructive long ocean waves in the tsunami frequency band: from observations and simulations towards a warning system"; http://www.izor.hr/messi), receives three different kind of data: (1) synoptic conditions from the Croatian Meteorological and Hydrological Service (DHMZ) operational atmospheric products, (2) high-resolution atmospheric and ocean model results provided by the Adriatic Sea and Coast (AdriSC) modelling suite (Denamiel et al., 2019), and (3) measurements from the MESSI observational network along the Adriatic coast. The synoptic data are used for a long-term qualitative forecast (at least a week) of meteotsunamigenic conditions through assessment of the synoptic meteotsunami index (Šepić et al., 2016). However, such an approach cannot be

This article is protected by copyright. All rights reserved.

Author Manuscript

used in quantitative meteotsunami hazard assessment and forecast, and is not further discussed in this paper.

The AdriSC modelling suite is composed of a basic module providing high-resolution regional atmospheric and ocean results for the entire Adriatic Sea and a dedicated meteotsunami module. The basic module uses a modified version of the Coupled Ocean-Atmosphere-Wave-Sediment-Transport (COAWST) modelling system developed by Warner et al. (2010), which couples (online) (1) the Regional Ocean Modeling System (ROMS) (Shchepetkin & McWilliams, 2005, 2009), with nested grids of 3-km (covering the entire Adriatic and Ionian Seas) and 1-km (covering the Adriatic Sea only), and (2) the Weather Research and Forecasting (WRF) model (Skamarock et al., 2005), with nested grids of 15-km (covering the central Mediterranean basin) and 3-km (identical to the 3-km ROMS grid). The dedicated meteotsunami module couples (offline) the WRF model – which downscales the hourly 3-km WRF results of the basic module to a 1.5-km resolution for a grid covering the entire Adriatic Sea, with the 2DDI ADvanced CIRCulation (ADCIRC) model (Luettich et al., 1991) using a mesh of up to 10 m resolution in the areas sensitive to meteotsunami hazard. In this deterministic configuration, the ADCIRC model is forced (1) every minute by the WRF 1.5-km wind and pressure fields, and (2) every hour by the ROMS 1-km sea-level fields (including tides). Every day at midnight, the next 48h hourly-forecast results from the COAWST run, as well as the 15min-forecast results from WRF 1.5-km and ADCIRC simulations for the next day, are published at http://www.izor.hr/adrisc.

The MESSI observational system currently encompasses a network of sensors set-up with a 1-min sampling rate and installed in areas where either the generation or the amplification of meteotsunamis are known to occur: eight air pressure sensors located in (1) Ancona, Ortona and

This article is protected by copyright. All rights reserved.

Author Manuscript

Author Manuscript

Vieste on the Italian coast, up to 200 km from any endangered location along the Croatian coastline, (2) Vis and Svetac in the middle of the Adriatic Sea and (3) Vela Luka, Stari Grad and Vrboska which are known sensitive harbors (Fig. 1) as well as two tide gauges located in the harbors of Vela Luka and Stari Grad (Fig. 1).

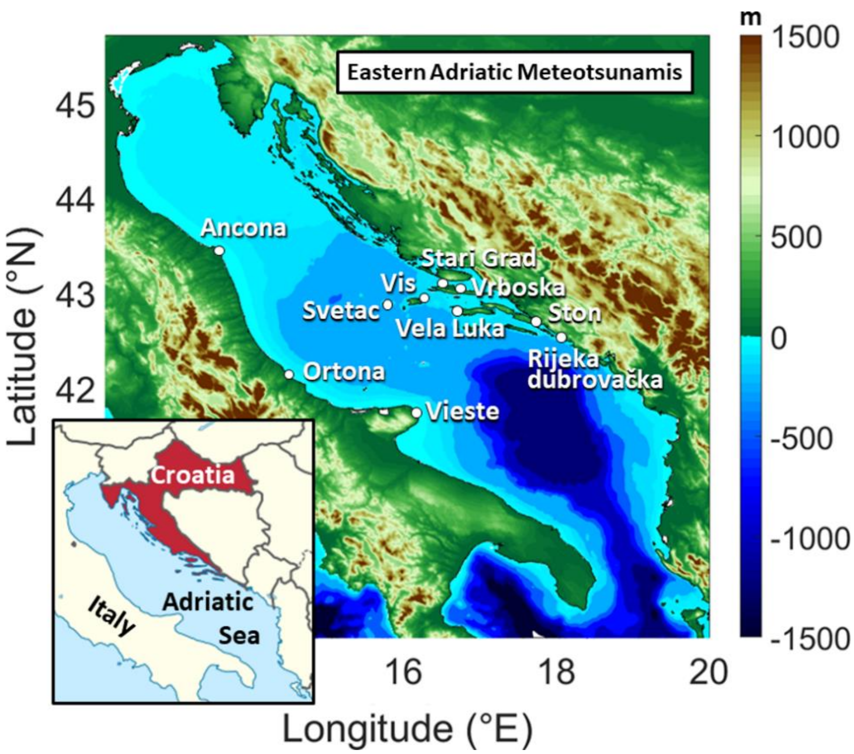

Figure 1. Locations of interest including measurement network along the Italian coast and in the middle of the Adriatic Sea (Ancona, Ortona, Vieste, Svetac and Vis) and sensitive harbor locations along the Croatian coast (Vela Luka, Stari Grad, Vrboska, Ston and Rijeka dubrovačka).

Within the CMeEWS, the extreme sea-level hazard assessment relies on the newly developed meteotsunami stochastic surrogate model. This model is based on generalized Polynomial Chaos Expansion (gPCE) methods (Xiu & Karniadakis, 2002; Soize & Ghanem, 2004) which, compared to sampling approaches (e.g. Monte Carlo simulations), are highly efficient for propagating the uncertainties of model inputs to outputs (e.g., Knio & Le Maître,

This article is protected by copyright. All rights reserved.

2006 and Najm et al., 2009 provide detailed discussions in the context of computational fluids applications). In this study, the stochastic surrogate model propagates the uncertainties from the meteorological input (i.e. the IGWs responsible for the meteotsunami generation) to the maximum sea-levels at different locations along the Croatian coastline. The surrogate model is based on polynomials expansions that decompose into deterministic coefficients and random orthogonal bases. The coefficients – which are the projection of the maximum meteotsunami elevation distribution onto each polynomial basis, are derived from a quadrature based approximation using numerical simulations undertaken with the ADCIRC model (identical to the one used in the AdriSC modelling suite) forced only by synthetic pressure disturbances (no wind, no tide). As described in Denamiel et al. (2018), the synthetic atmospheric pressure forcing is split into (1) a mean atmospheric pressure component (P_0) assumed constant over the entire Adriatic Sea and (2) a stochastic gravity wave component (P_{GW}) depending on 6 stochastic parameters – start location $\left(y_0\right)$, direction $\left(\theta\right)$, speed $\left(c\right)$, period $\left(T\right)$, amplitude $\left(P_A\right)$ and width $\left(d\right)$ of the disturbance. These 6 parameters are assumed to have uniform distributions and are defined on the following intervals: $y_0 \in \left[41.25^o, 43.65^o\right]$, $\theta \in \left[-\frac{\pi}{3}, \frac{\pi}{2}\right]$, $c \in \left[15\text{m s}^{-1}, 40\text{m s}^{-1}\right]$, $T \in \left[300\text{s}, 1800\text{s}\right]$, $P_A \in \left[50\text{Pa}, 400\text{Pa}\right]$ and $d \in \left[30km, 150km\right]$. Examples of synthetic gravity wave spatial and temporal properties can be visualized as supporting information (Fig. S1). Practically, as the input parameters are assumed to be uniformly distributed, (1) the delayed Gauss-Patterson sparse grid method (Smolyak, 1963; Novak et al., 1999; Burkardt, 2014) is applied to automatically select all the combined values of the 6 stochastic parameters of the synthetic pressure forcing and thus to define the number of simulations (in this study 4161 as the gPCE is defined for polynomial degrees up to 6) used to

Author Manuscript

This article is protected by copyright. All rights reserved.

derive the polynomial coefficients, while (2) the random orthogonal bases are built with Legendre polynomials. The meteotsunami hazard forecast is illustrated in Figure 2 and is based on the meteotsunami stochastic surrogate model receiving atmospheric pressure field input from both (1) the WRF 1.5-km next day forecast results (brown box, Fig. 2) and (2) the real-time transmitted observations from Ancona, Ortona, Vieste, Svetac and Vis stations (green box, Fig. 2).

2.2 Operational mode

Every day, as soon as the WRF 1.5-km 1-min forecast results are available – which is at least 30h before any potential meteotsunami event (M) can occur, the high-pass filtered (with a 2h cutoff period) mean sea-level pressure (i.e. P_{GW} for meteotsunami events) is automatically extracted (AdriSC Forecast step, Fig. 2). Then the maximum temporal rate of change (over a 4-min interval T_4) of this filtered pressure – i.e. $R_M = \max_{T_4} \frac{\partial P_{GW}}{\partial T_4}$, is derived at each WRF 1.5-km grid sea point. Such a condition has been proven to be efficient for the detection of meteotsunamigenic disturbances (Vilibić et al., 2016). No later than 28h before any meteotsunami event, the spatial coverage (in percentage) of the WRF 1.5-km grid sea points with a maximum temporal rate above 20Pa per 4-min interval ($R_M \geq 20$) is calculated (Automatic Detection step, Fig. 2). If this coverage exceeds 5%, a potential meteotsunami has been detected (event mode of the warning) and an automatic email – including a figure of the distribution of $R_M \geq 20$, is sent to the AdriSC team (red box, Fig. 2). The threshold of 5% is prescribed, being based on the analysis of recent meteotsunami events in which reproduction by the AdriSC modelling suite has been included (Denamiel et al., 2019). Otherwise (silent mode of the

Author Manuscript

This article is protected by copyright. All rights reserved.

warning), at this stage, it is assumed that no meteotsunami will occur in the next forecasted day (blue box, Fig. 2).

Author Manuscript

This article is protected by copyright. All rights reserved.

Author Manuscript

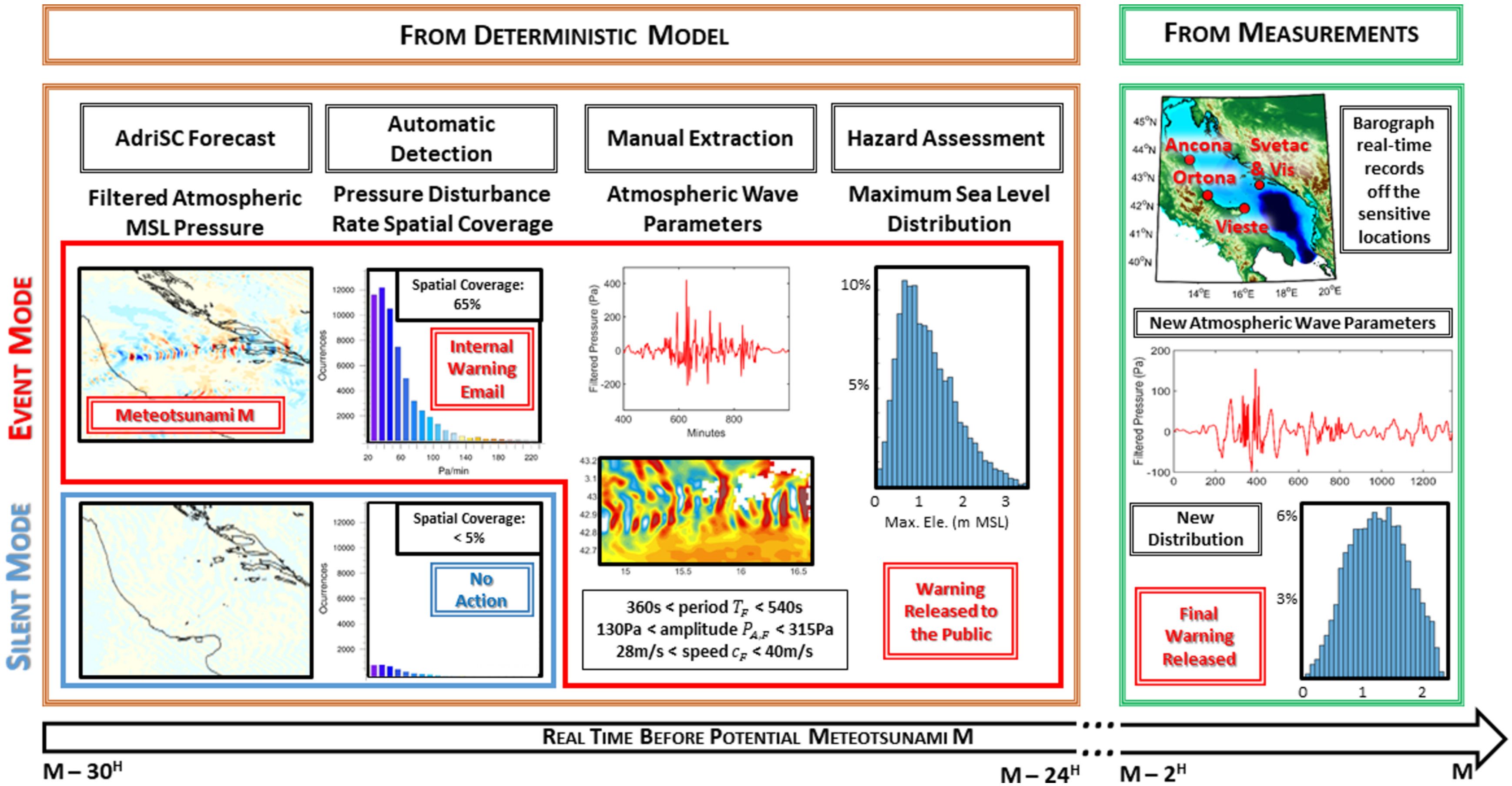

Figure 2. Operational meteotsunami hazard forecast within the CMeEWS, based on atmospheric pressure field input from both (1) the deterministic model results (brown box) and (2) the measurements (green box). Every day, at least 30h before any meteotsunami event, the high-pass filtered pressure is extracted from the AdriSC forecast and used to automatically detect meteotsunamis by checking the spatial coverage of the values above 20Pa per 4-min interval of the maximal pressure temporal rate. If this coverage is below 5% then no meteotsunami is forecasted (blue box) – "silent" warning mode, otherwise a potential meteotsunami M is foreseen to occur (red box) – "event" warning mode, and an email is sent to the AdriSC team. At least 24h before the potential meteotsunami M occurs, the first forecast of hazard assessment is derived from the stochastic surrogate model used with ranges of pressure wave parameters manually extracted from the modelled filtered pressure. Finally, when the real-time observations become available, the hazard assessment is updated with new parameters extracted from the measurements.

This article is protected by copyright. All rights reserved.

Author Manuscript

In case of automatic meteotsunami detection, no later than **27h before any meteotsunami event**, the filtered pressure field is visualized and analyzed by the AdriSC team. If the detected pressure disturbance is recognized as an atmospheric pressure gravity wave, the ranges of variation of the forecasted wave parameters including a $\pm 10\%$ of the parameter interval of definition – latitude of origin $\left(y_{0,F} \pm 0.24°N\right)$, direction of propagation $\left(\theta_F \pm 0.26rad\right)$, amplitude $\left(P_{A,F} \pm 35Pa\right)$, period $\left(T_F \pm 150s\right)$ and width $\left(d_F \pm 12000m\right)$, are manually estimated from the WRF 1.5-km 1-min filtered air pressure results (Manual Extraction step, Fig. 1). To the best of the author knowledge, the technology to automatically detect and extract the parameters of the atmospheric disturbances driving the Adriatic Sea meteotsunamis is yet to be developed and thus, for the moment, human intervention is unfortunately required in the early warning system. As the errors associated with manually deriving the speed of the gravity waves $\left(c_F\right)$ are quite large, this parameter is always taken on its full range of definition $\left[15\text{m s}^{-1}, 40\text{m s}^{-1}\right]$. At least 24h before the forecasted meteotsunami event, the meteotsunami stochastic surrogate model – based on generalized Polynomial Chaos Expansion (gPCE), is used to deduce the meteotsunami maximum elevation distributions at different locations of interest (Hazard Forecast step, Fig. 2) via the user friendly interface developed in Matlab (Fig. 3). These distributions are derived from 20000 random combinations of the six uniformly distributed input variables selected in the range of the extracted parameters. In order to produce a conservative estimate of the final maximum elevation expected at the locations of interest, (1) the surrogate model results below 0.1m are ignored as irrelevant for meteotsunami hazard, and (2) the maximum tidal elevation of the forecasted 24h period is added to the results of the stochastic surrogate model.

This article is protected by copyright. All rights reserved.

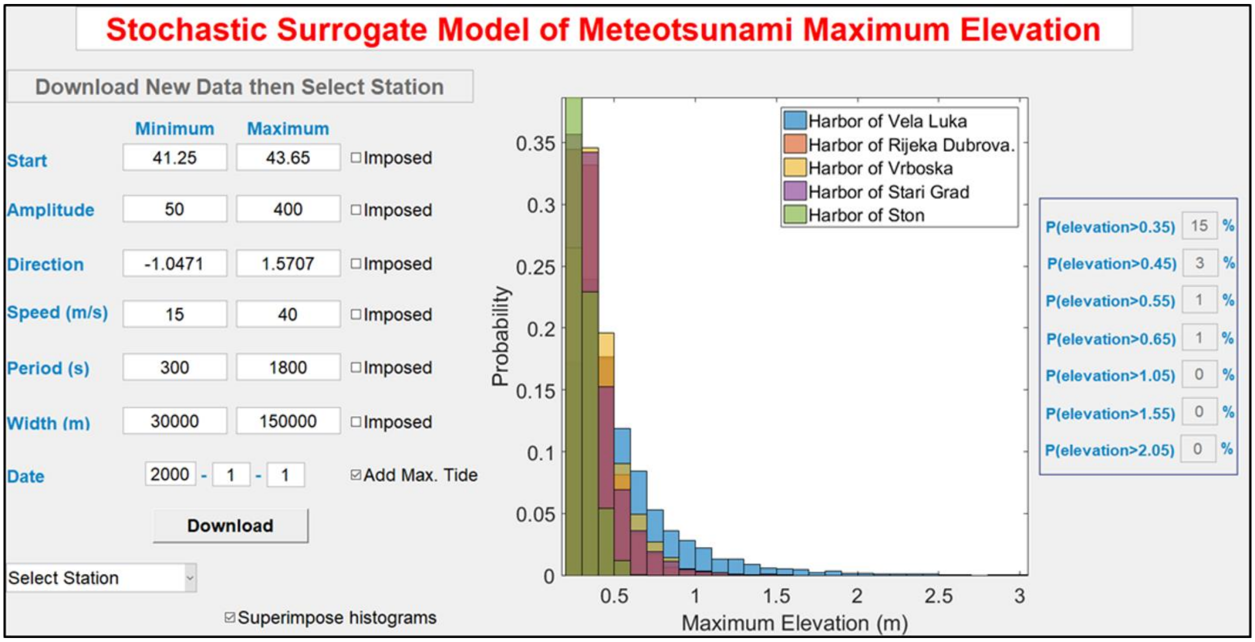

Figure 3. User friendly interface of the stochastic surrogate model of meteotsunami maximum elevation developed in Matlab.

The maximum elevation distribution depending on the interval of definition of the atmospheric wave parameters is generated and a first warning provides, at each location of interest, (1) the probability of the expected maximum elevation derived from the surrogate model, and (2) the deterministic maximum elevation from the ADCIRC model run, which is also taken into account during the decision process for timely managing the hazard. Finally, it is planned that once the early warning system will be fully operational (24/7 watch or fully automated procedure), in the 2h period before the forecasted meteotsunami event (i.e. the estimated time for the atmospheric disturbances to cross the Adriatic Sea from the Italian cost), the 1-min air pressure measurements from Ancona, Ortona, Vieste, Svetac and Vis will be analyzed by the AdriSC team and, if any pressure gravity wave is detected, amplitude and period will be extracted from the observations $\left(P_{A,M}, T_M\right)$. These parameters will then be used as constant values in the stochastic surrogate model and new maximum elevation distributions will be produced with 20000 random

Author Manuscript

This article is protected by copyright. All rights reserved.

combinations of the three remaining uniformly distributed input variables selected in the range of the parameters extracted from the model results $\left(y_{0,F}, \theta_F, d_F\right)$. The final meteotsunami warning using the updated distribution of the maximum elevation (including maximum tidal elevation) will then be ready to be published and accessible to users.

3 Evaluation of the meteotsunami early warning system

3.1 Evaluation against historical events

The first evaluation of the CMeEWS is performed against well-recorded events that took place, before the early warning system became operational, at five locations of interest: Vela Luka, Rijeka dubrovačka, Stari Grad, Vrboska and Ston (Fig. 1). In 2014, two strong events happened at the end of June (Šepić et al., 2016), with reported maximum elevations of 1.5m in Vela Luka, 0.5m in Stari Grad, 0.75m in Vrboska and 1.75m in Rijeka dubrovačka on the 25th of June, and of 0.5m in Ston on the 26th of June. In summer 2017, tsunami-like waves were also generated and observed in Stari Grad on the 28th of June (maximum elevation of 0.75m; Denamiel et al., 2019) as well as the 30th of June during the night (http://www.izor.hr/meteotsunami; maximum elevation of 0.32m measured at 18:30 UTC) and in Vrboska on the 1st of July (maximum elevation of about 0.75m). Finally, on the 31st of March 2018, a meteotsunami wave with maximum reported sea elevation of 0.5m flooded Stari Grad (Denamiel et al., 2019). For five of these events, the deterministic results of the AdriSC Meteotsunami Forecast component have already been evaluated against a set of 48 air pressure sensors and 19 tide gauges (Denamiel et al., 2019). This evaluation highlighted that the WRF 1.5-km model used in the AdriSC modelling suite presents some skills in forecasting the internal gravity waves (IGWs) responsible for the observed meteotsunamis (i.e. the IGWs were always forecasted by the model but their intensity or direction of propagation may not have been

Author Manuscript

This article is protected by copyright. All rights reserved.

reproduced perfectly). However, it also revealed that the slightest shift in location of the modelled atmospheric disturbances resulted in the incapability of the ADCIRC model to reproduce the observed meteotsunamis in the deterministic mode of the forecast. The stochastic approach was thus developed to counter these shortcomings.

In this study, the stochastic surrogate model of the CMeEWS is also tested against these five events in order to assess its capability to provide relevant warning to the public. In addition, as the pressure sensors only became operational at the end of 2017, the atmospheric wave parameters used in the stochastic surrogate model are only extracted from the WRF 1.5-km 1-min high-pass filtered atmospheric pressure results. Finally, the meteotsunami impact highly depends on the location of interest because (1) observations have shown that extreme meteotsunami elevations present significant spatial variations in the eastern Adriatic Sea (Šepić et al, 2016), and (2) flooding – the main hazard caused by meteotsunamis, depends on the geomorphology/harbor design (Denamiel et al., 2018). In addition, due to the design of the surrogate model (i.e. uniform prior distribution of the parameters), a majority of the stochastic combinations lead to small oscillations (maximum elevations below 0.2m as seen in fig. 3) while only about 10% lead to meteotsunami conditions. In this study it is thus assumed that flooding occurs when at least 10% of the stochastic surrogate model maximum elevations reach more than 1.05m in Vela Luka, 0.65m in Rijeka dubrovačka, 0.55m in Vrboska, 0.45m in Stari Grad and 0.35m in Ston. These threshold values are prescribed considering the resilience of the coastline in these locations (e.g. the salt plant located in Ston is the least resilient to strong sea-level changes and meteotsunami waves), which in turn is largely defined by the real meteotsunami hazard (e.g. the community of Vela Luka is the most resilient to meteotsunami hazard, as they were hit by the strongest meteotsunami events along the Croatian coastline, Orlić, 2015).

This article is protected by copyright. All rights reserved.

Author Manuscript

Author Manuscript

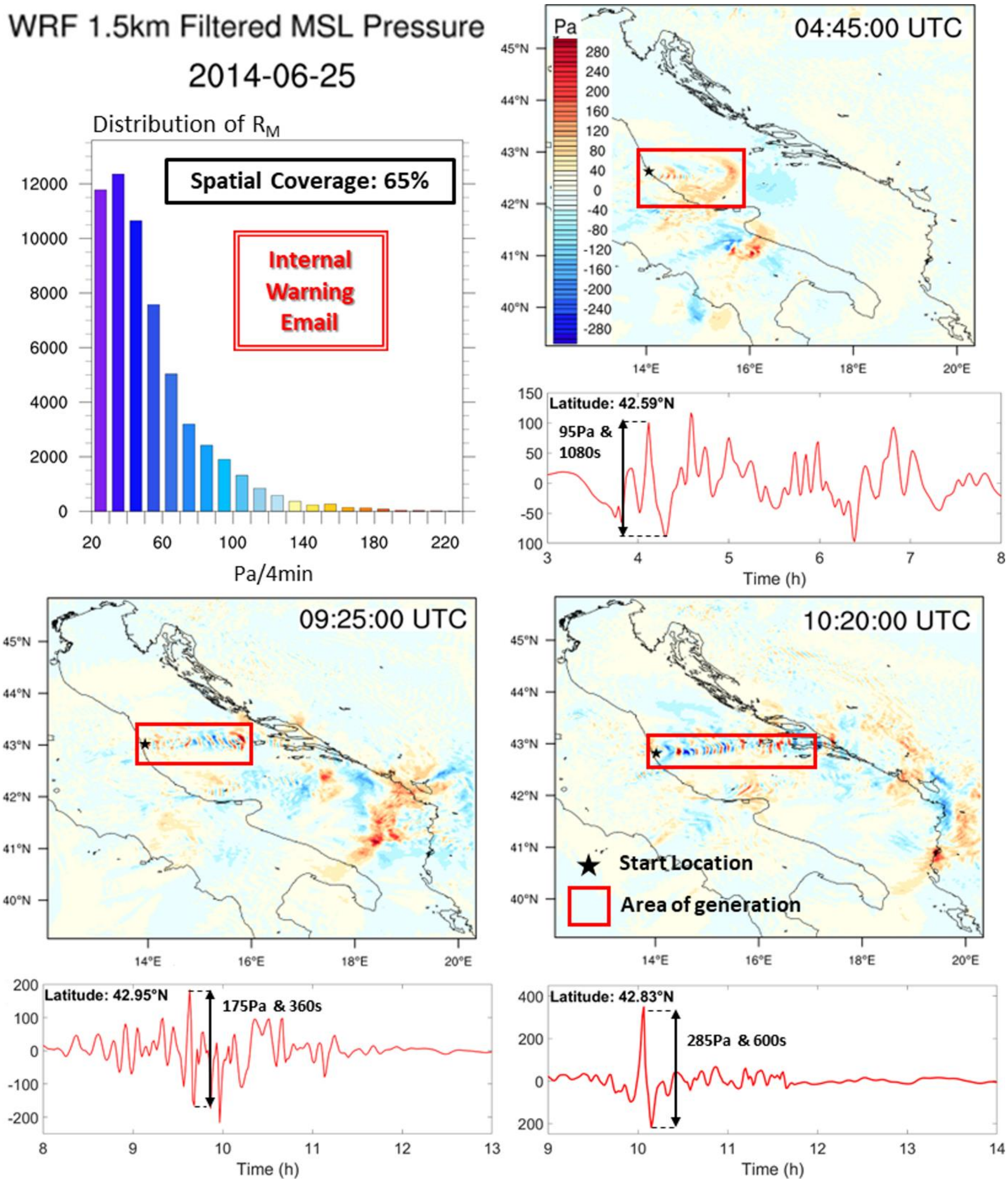

Figure 4. Meteotsunami event of the 25th of June 2014: distribution and spatial coverage of the maximum temporal rate of change $\left(R_M\right)$ and associated spatial and temporal variations of the three atmospheric gravity waves extracted from the WRF 1.5-km forecast model. Time series of filtered MSL pressure are extracted at the start location of the three different disturbances (black stars) and direction of propagation is given by the orientation of the red boxes representing the area of generation of the meteotsunami waves.

This article is protected by copyright. All rights reserved.

Table 1. Input and output of the surrogate model during the five events used in the evaluation against historical events: (1) range of atmospheric gravity wave parameters (start location, amplitude, direction, period and width) extracted from the WRF 1.5-km forecast model results and (2) probability (in percent) of the maximum meteotsunami elevation surpassing the flooding threshold defined at five different locations (Vela Luka, Rijeka dubrovačka – R. dubro., Stari Grad, Vrboska and Ston). When the probabilities are above or equal to 10% (highlighted in bold), the meteotsunami warning is triggered. In addition, probabilities at locations at which flooding has been reported by eye-witnesses during the events are highlighted in red.

			25/06/14	**26/06/14**	**28/06/17**	**01/07/17**	**31/03/18**
Range of the input parameters	**Latitude (°N)**	Minimum	42.34	41.25	42.24	41.25	42.03
		Maximum	43.20	41.70	43.13	42.81	42.79
	Amplitude (Pa)	Minimum	60	255	85	100	85
		Maximum	320	340	185	275	215
	Direction (rad)	Minimum	-0.17	0.08	-0.17	0.35	0.26
		Maximum	0.35	0.60	0.70	1.04	0.78
	Period (s)	Minimum	300	330	1290	300	330
		Maximum	1230	630	1800	1410	1350
	Width (km)	Minimum	30	30	88	30	30
		Maximum	54	54	112	92	54
Probability (%)	**Vela Luka**	$P(\xi_{\max} \geq 1.05\text{m})$	**12**	**10**	**20**	7	**19**
	R. dubro.	$P(\xi_{\max} \geq 0.65\text{m})$	**17**	1	5	3	**12**
	Stari Grad	$P(\xi_{\max} \geq 0.45\text{m})$	**25**	0	**15**	2	**25**
	Vrboska	$P(\xi_{\max} \geq 0.55\text{m})$	**10**	**16**	**50**	**10**	**23**
	Ston	$P(\xi_{\max} \geq 0.35\text{m})$	7	**27**	7	2	**11**

Author Manuscript

This article is protected by copyright. All rights reserved.

Author Manuscript

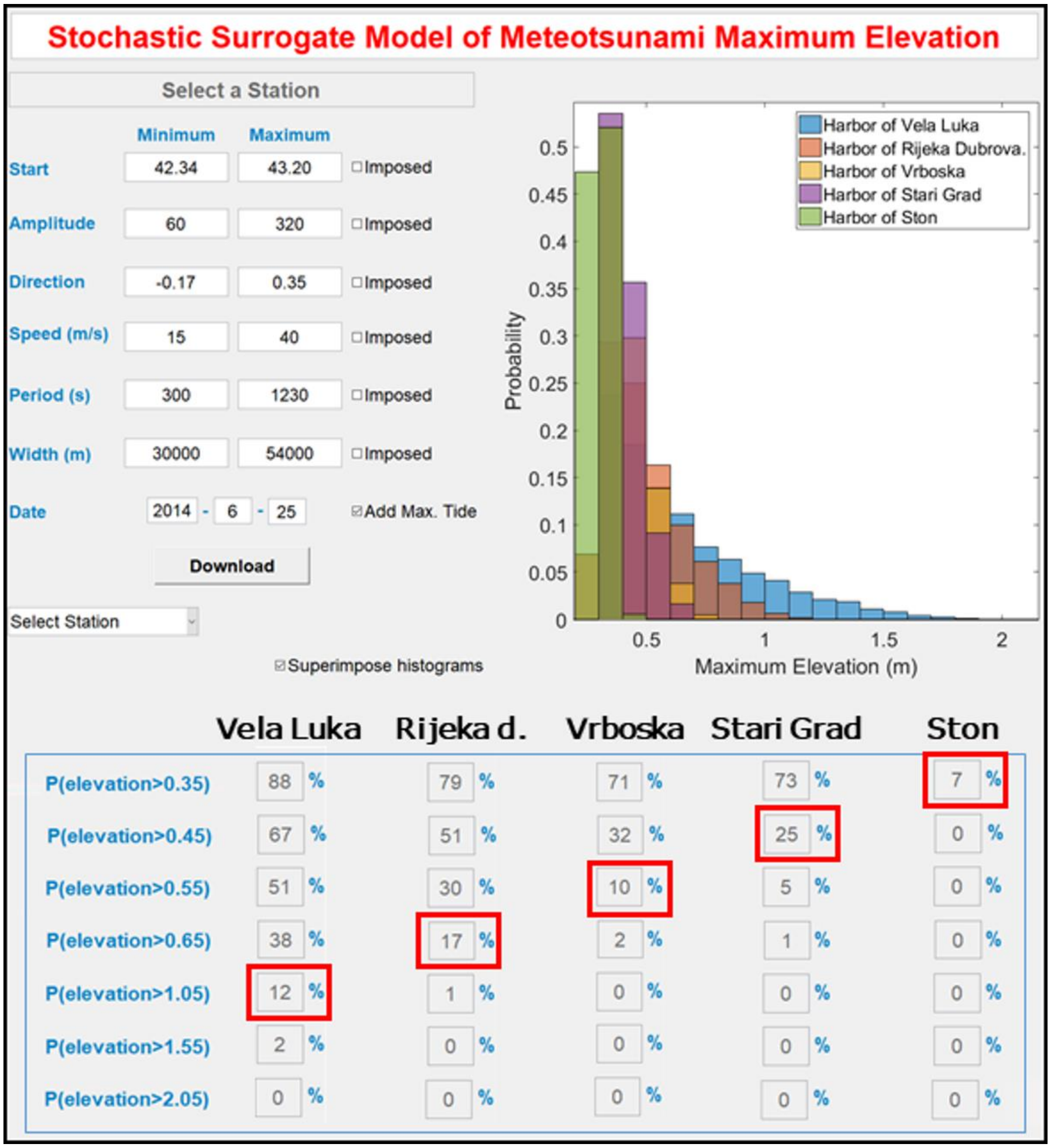

Figure 5. Maximum elevation distribution derived with the meteotsunami surrogate model at the five locations of interest (Vela Luka, Rijeka dubrovačka, Stari Grad, Vrboska and Ston) for the 25th of June 2014 event.

In addition, as the thresholds dependent on the meteotsunami impact at the five studied locations, their values will most probably be re-evaluated in the near-future when more well-documented meteotsunami events in the eastern Adriatic will become available.

This article is protected by copyright. All rights reserved.

For each of the five meteotsunami events used in the evaluation, the distribution and spatial coverage of the maximum temporal rate of change above 20Pa per 4 minutes $\left(R_M\right)$ as well as the different IGWs generated by the WRF 1.5-km model are analyzed. An example of this data is presented in Figure 4 for the 25th of June 2014 event (figures for other events are given as supporting information S2 to S5). As the spatial coverage of $R_M \geq 20$ is above 5% for all the events, the switch of the warning system to the event mode would have been triggered in operational conditions. The intervals of the atmospheric disturbance parameters $\left(y_{0,F}, \theta_F, P_{A,F}, T_F, d_F\right)$ defined with a $\pm 10\%$ margin to cover all possible IGW conditions forecasted during the 24-h period of the event are thus presented in Table 1. The probabilities of the maximum meteotsunami elevation $\left(\xi_{\max}\right)$ surpassing the flooding threshold defined at the five locations of interest are extracted from the surrogate model results and also presented in Table 1. In addition, an example of the surrogate model results is presented Figure 5 for the 25th of June 2014 event (figures for other events are given as supporting information S6 to S9). Given the flooding criteria chosen in this study, in operational mode, the meteotsunami warnings would have been triggered as follow:

- the 25th of June 2014: for Vela Luka, Rijeka dubrovačka, Vrboska and Stari Grad, which all have been reported to be flooded (Šepić et al., 2016); this is in accordance with the forecasted deterministic ADCIRC maximum elevation results (1.45m in Vela Luka, 0.80m in Rijeka dubrovačka, 0.65m in Stari Grad and 0.55m in Vrboska),
- the 26th of June 2014: for Vela Luka, Vrboska and Ston but, following eyewitness reports, only Ston experienced flooding which was accurately forecasted with the deterministic ADCIRC maximum elevation of 0.55m,

This article is protected by copyright. All rights reserved.

- the 28th of June 2017: for Vela Luka, Stari Grad and Vrboska but, following eyewitness reports, only Stari Grad experienced flooding; the deterministic results obtained with the ADCIRC model forecasted an elevation of only 0.35m in Stari Grad which would not have been enough to cause flooding,
- the 1st of July 2017: for Vrboska, which was the only place flooded during this event; the deterministic ADCIRC model forecasted 1m maximum elevation in Vela Luka but did not captured proper meteotsunami amplification in Vrboska,
- the 31st of March 2018: for all the five locations but, following eyewitness reports, only Stari Grad experienced flooding; the deterministic ADCIRC model did not reproduce at all this event (only 0.25m forecasted in Stari Grad).

In summary, for the five studied historical events, the surrogate model of meteotsunami maximum elevation is capable of forecasting the meteotsunami hazard in the areas that were flooded, which was not always the case of the deterministic ADCIRC model (Denamiel et al., 2019). Unfortunately, for many events, it also predicts flooding in areas where no meteotsunami impact was reported.

3.2 Evaluation in operational mode

Since September 2018, the CMeEWS is tested in operational mode but meteotsunami warnings are not yet released to the public. After nearly a year of run, meteotsunami hazard forecasts were performed with the surrogate model forced by both deterministic model results and measurements, for several events presenting the required meteotsunamigenic conditions (Table 2).

The first event occurred on the 29th of October 2018 in the evening during the Vaia storm, but was not publicly reported as a meteotsunami. The switch of the warning system to

This article is protected by copyright. All rights reserved.

Author Manuscript

event mode was triggered by (1) a 32% spatial coverage for $R_M \geq 20$ and (2) the analysis of the WRF 1.5-km filtered MSL pressure which revealed the presence of several high-frequency atmospheric disturbances travelling northwards from Vieste to the Croatian coastline (as can be seen in Figure **S10** of the supporting information). However, only relatively small sea-level oscillations were deterministically forecasted with the ADCIRC model in the studied harbors along the track of the pressure disturbance (Vela Luka, Stari Grad and Vrboska). The first hazard forecast, based on the numerical results (Fig. S9), triggered the meteotsunami warning for all the locations except Rijeka dubrovačka (R1, Table 2 and Fig. S11 of the supporting information). The analysis of the filtered pressure measured at Vieste and Svetac (Fig. 6) – which were the stations the closest to the forecasted track of the pressure disturbances, showed that several IGWs of about 80Pa of amplitude and 10min of period were recorded between 18:00 and 22:00 UTC.

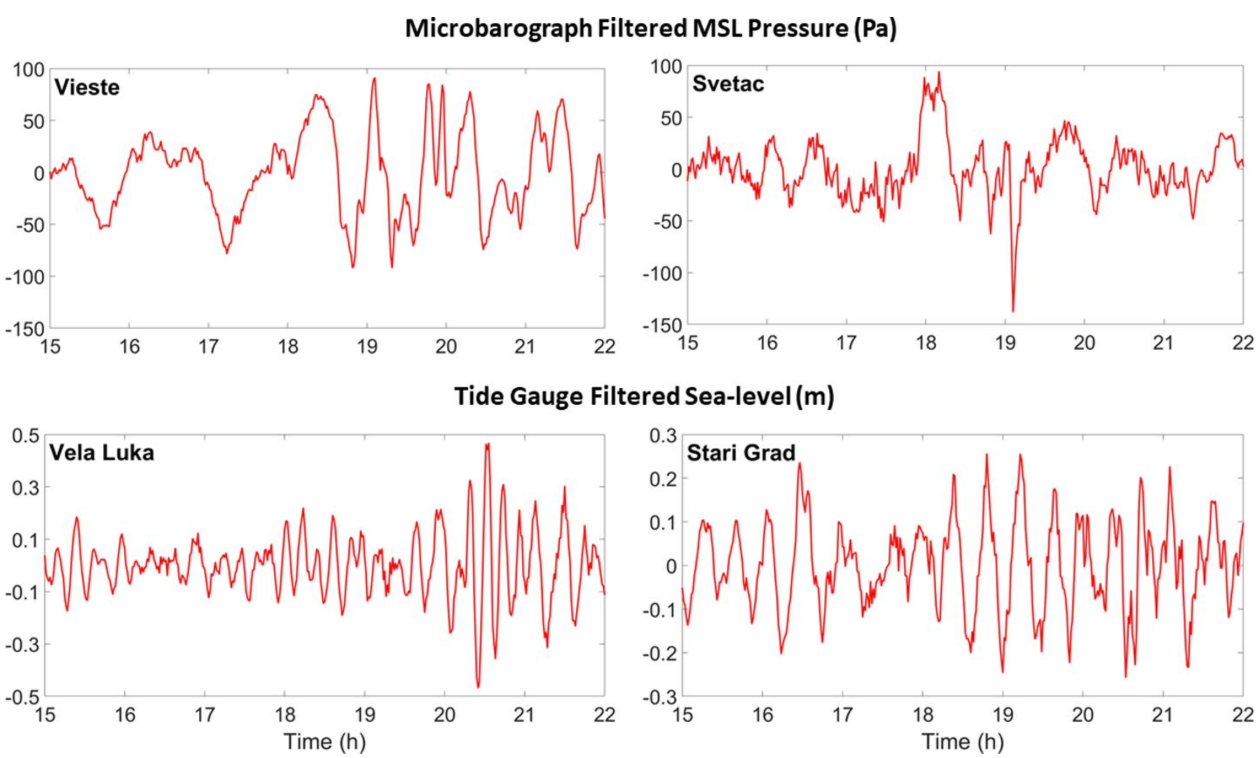

Figure 6. Available 1-min measurements (high-pass filtered with a 2h cutoff period) along the

This article is protected by copyright. All rights reserved.

forecasted track of the atmospheric disturbances during the 29th of October 2018: mean sea-level pressure at Vieste and Svetac and sea-level at Vela Luka and Stari Grad.

Author Manuscript

This article is protected by copyright. All rights reserved.

Author Manuscript

Table 2. As Table 1 but for the events that were detected since the warning system became operational in late 2018. R1 stands for a meteotsunami hazard forecast forced with input parameters extracted from the WRF-1.5km numerical model, while R2 hazard forecast uses air pressure amplitude and period extracted from the measurements and imposed as constant values, if a pressure disturbance is captured by the microbarographs. providing the final meteotsunami hazard.

			29/10/18		**09/07/19**		**10/07/19**	**02/08/19**
			R1	R2	R1	R2	R1	R1
Range of the input parameters	**Latitude (°N)**	Minimum	41.25		43.40		43.17	42.54
		Maximum	41.49		43.65		43.65	43.02
	Amplitude (Pa)	Minimum	86	80	175	135	172	53
		Maximum	173		245		400	123
	Direction (rad)	Minimum	1.31		-0.26		-0.26	-0.26
		Maximum	1.57		0.26		0.26	0.26
	Period (s)	Minimum	390	600	1530	1800	750	450
		Maximum	870		1800		1230	750
	Width (km)	Minimum	30		38		48	38
		Maximum	54		62		72	62
Probability (%)	**Vela Luka**	$P(\xi_{\max} \geq 1.05\text{m})$	**10**	6	0	0	0	1
	R. dubro.	$P(\xi_{\max} \geq 0.65\text{m})$	7	1	1	1	1	**26**
	Stari Grad	$P(\xi_{\max} \geq 0.45\text{m})$	**29**	**14**	**19**	**29**	2	**21**
	Vrboska	$P(\xi_{\max} \geq 0.55\text{m})$	**29**	**25**	8	**20**	1	0
	Ston	$P(\xi_{\max} \geq 0.35\text{m})$	**11**	5	0	0	0	**10**

This article is protected by copyright. All rights reserved.

After the hazard forecast was updated based on these measured values, the warning only remained for Stari Grad and Vrboska (R2, Table 2 and Fig. S12 of the supporting information). After the event, filtered sea-level measured at Vela Luka and Stari Grad (Fig. 6) revealed that high-frequency oscillations with the respective periods of about 12min and 25min occurred at both locations and generated the respective maximum elevations of 0.48m at 20:30 UTC and 0.26m at approximately 18:45 UTC. If the maximum tidal elevation (about 0.16m for both locations during this event) is added, then the total elevation reached 0.64m in Vela Luka, which is not enough to generate flooding, and 0.42m in Stari Grad which is slightly below the 0.45m threshold that is used for the meteotsunami hazard warning. Unfortunately, no sea-level measurements were available in Vrboska and, similarly to Stari Grad, even if a small meteotsunami had occurred, it is unlikely that its effect could be visually distinguished from the impact of the Vaia storm.

The next events all took place during summer storms in July and August 2019, when unfortunately, the Ancona microbarograph stopped transmitting data. Between the 9th and the 10th of July 2019, the Adriatic region experienced severe storms which brought heavy rains, hurricane force downbursts, tornadoes and the largest hailstorm ever recorded to date along the Italian coast. For both days the event mode of the early warning system was triggered as (1) the spatial coverage for $R_M \geq 20$ reached 22% and 44%, mostly due to the passage of the storm, and (2) the analysis of the WRF 1.5-km filtered MSL pressure showed the presence of high-frequency atmospheric disturbances with amplitudes greater than 150Pa travelling eastwards from Ancona to the Croatian coastline (as can be seen in Figures S13 and S14 of the supporting information).

Author Manuscript

This article is protected by copyright. All rights reserved.

Author Manuscript

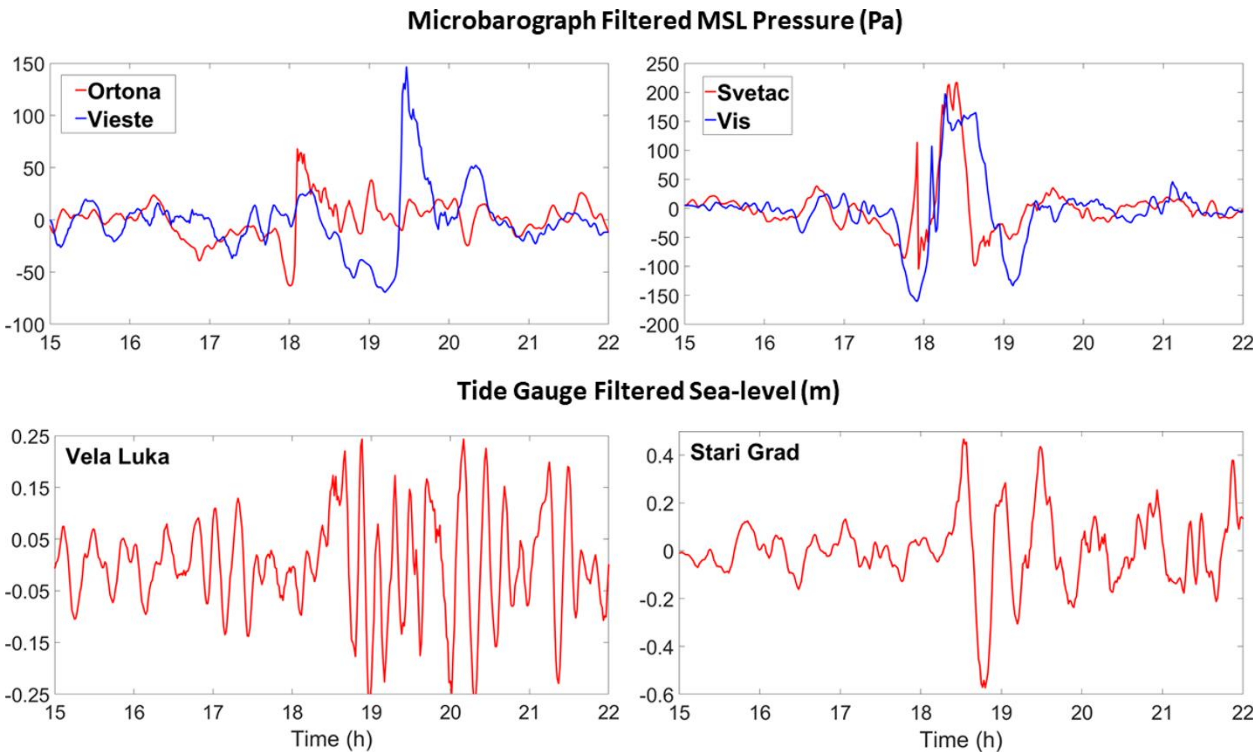

Figure 7. Available 1-min measurements (high-pass filtered with a 2h cutoff period) along the forecasted track of the atmospheric disturbances during the 9th of July 2019: mean sea-level pressure at Ortona, Vieste, Svetac and Vis and sea-level at Vela Luka and Stari Grad.

However, for these two days, similarly to the Vaia storm, the deterministic ADCIRC model only forecasted relatively small oscillations in the harbors of Vela Luka, Stari Grad and Vrboska located along the track of the pressure disturbances. For the 9th of July 2019, the first hazard forecast, based on numerical model results, triggered the meteotsunami warning in Stari Grad (R1, Table 2 and Fig. **S15** of the supporting information). In addition, the analysis of the filtered pressure measured at Ortona, Vieste, Svetac and Vis stations (Fig. 7) clearly showed an atmospheric disturbance of about 135Pa and 30min period travelling eastward from Svetac to Vis between 17:30 and 18:30 UTC. As both Ortona and Vieste are located south from the forecasted track of the pressure disturbances, the pressure waves recorded at these stations were

This article is protected by copyright. All rights reserved.

assumed to be incapable to affect Stari Grad harbor where the warning was issued. Based on the final hazard assessment (R2, Table 2 and Fig. S16 of the supporting information) updated with the values extracted from the Svetac and Vis stations, the Stari Grad warning was confirmed and an additional warning was triggered for Vrboska. During the evening of the 9th of July 2019, a meteotsunami occurred in the harbor of Stari Grad, where the promenade was flooded (https://www.dalmacijadanas.hr/meteoroloski-tsunami-na-hvaru-more-se-povuklo-za-vise-od-metra). The analysis of the filtered sea-levels in Stari Grad (Fig. 7) confirmed the presence of a 1.05m height and 25min period meteotsunami wave just before 19:00 UTC. During the event, the measured maximum elevation reached 0.47m which is, even without adding the maximum tidal elevation, beyond the threshold value of 0.45m defined for meteotsunami warning. Sea-level oscillations were also recorded in Vela Luka (Fig. 7), but the maximum elevation never surpassed 0.25m. Finally, no meteotsunami was reported in Vrboska and thus the warning was most probably too conservative for this location. For the 10th of July 2019, the forecasted meteotsunami conditions were similar to the ones obtained from the previous day, except concerning the periods of the disturbances which were all below 18min instead of the measured 30min. As meteotsunami are extremely sensitive to the period of the atmospheric disturbances, no warning was triggered by the hazard forecast based on these numerical results (R2, Table 2 and Fig. S17 of the supporting information). In addition, the monitoring of the air pressure measurements did not show any disturbance with period greater than 18min and no meteotsunami was reported in the studied locations.

Two more storms took place in the Adriatic Sea during the 13th and the 28th of July 2019 (not presented in this study) and both triggered the event mode of the warning system, but conditions for these storms were extremely similar to the 10th of July 2019 event and the hazard

This article is protected by copyright. All rights reserved.

Author Manuscript

forecast based on both numerical results and measurements did not trigger any meteotsunami warning.

Finally, the last event occurred the 2nd of August 2019 just before a storm that swept the eastern Adriatic coast, where falling trees blocking roads, damaged power distribution lines and flooding were reported in the media. The event mode was triggered by (1) a 19% spatial coverage for $R_M \geq 20$ and (2) the analysis of the WRF 1.5-km filtered MSL pressure which revealed that a high-frequency atmospheric disturbance was travelling eastwards around 10:00 UTC in the middle of the Adriatic (about 42.77°N of latitude), from the Italian to the Croatian coasts (as can be seen in Figure S18 of the supporting information). The forecasted meteotsunami hazard based on these numerical results was quite high and warnings were triggered for Rijeka dubrovačka, Stari Grad and Ston (R1, Table 2 and Fig. S19 of the supporting information). Similarly to the other events, the deterministic results of the ADCIRC model only forecasted some oscillations of small amplitude in the harbors of interest. Due to technical problems the Ortona and Vela Luka stations were not transmitting data during this event, thus the analysis of the filtered pressure was based on measurements at Svetac and Vis (Fig. 8). Interestingly, some disturbances were indeed travelling eastwards during the 2nd of August between 10:00 and 12:00 UTC. However, their amplitude was below 50Pa and they were not capable of generating strong oscillations and/or flooding along the Croatian coast. The warnings were thus canceled and in fact no meteotsunami was reported for this event. Finally, the biggest atmospheric disturbance – which generated some moderate oscillations (about 0.15m of amplitude) in the harbor of Stari Grad, as can be seen in the filtered sea-level data (Fig. 8) – was recorded between 20:00 and 22:00 UTC during the peak of the storm.

This article is protected by copyright. All rights reserved.

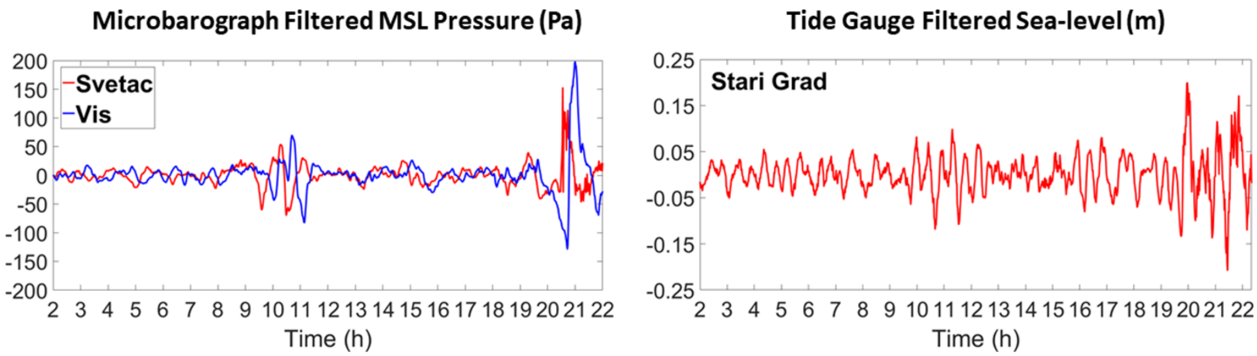

Figure 8. Available 1-min measurements (high-pass filtered with a 2h cutoff period) along the forecasted track of the atmospheric disturbances during the 2nd of August 2019: mean sea-level pressure at Svetac and Vis and sea-level at Stari Grad.

For this event, the assessment of the meteotsunami hazard was first largely overestimated due to the deterministic forecast of pressure disturbances capable of generating strong sea-level oscillations in the eastern Adriatic but, as the measured pressure disturbances were far smaller than expected, no meteotsunami occurred.

The evaluation of the CMeEWS in operational mode highlights that the microbarograph network plays a crucial role in terms of delivering the final warnings and confirms that the surrogate model forecasts the meteotsunami hazard in a conservative way even during storms events which, in the eastern Adriatic, are not the classical generation mechanism of the meteotsunamigenic pressure disturbances.

4 Discussion and conclusions

Notwithstanding major research efforts, the scarcity of the measurements and the reliability of the numerical models in meteotsunami studies are still major restrictions for hazard assessment and forecast, and even more for risk management (e.g. for the determination of a 100-year meteotsunami event). Based on lessons from river flooding hazard warning systems

Author Manuscript

This article is protected by copyright. All rights reserved.

designed and evaluated in hydrological studies (e.g. Beven, 2006; Sivakumar, 2008), two major conclusions can be drawn: (1) the promotion of uncertainty analysis of measurements and modelled results is of crucial importance for hazard assessment and forecast, and (2) the effectiveness of the warning systems is not determined only by the predictive accuracy of the models, but also by the lead time and the available social response set.

The presented prototype of meteotsunami early warning system combining deterministic and stochastic hazard assessment was designed to address such concerns. In particular, the very first use of a gPCE-based surrogate model to derive atmospherically-driven extreme sea-level hazard was motivated by the successful application of such methods for uncertainty quantification in a wide range of areas including mechanics, engineering, water resources and geosciences (e.g. Foo et al., 2007; Rupert & Miller, 2007; Giraldi et al., 2017). The main advantages of this kind of approach are (1) the propagation of the uncertainties associated with the atmospheric disturbances (e.g. location, direction, speed) to the maximum elevation results, (2) the potentiality of using both deterministic forecast results and measurements to provide the surrogate model input parameters, and (3) the few minutes of computation needed to assess, with a large number of samples and no additional deterministic simulation, the hazard of any studied event (e.g. meteotsunami). However, the main disadvantages are that the surrogate model (1) only relies on ocean numerical results forced by synthetic atmospheric disturbances (e.g. idealized pressure waves), and (2) requires a large number of synthetic simulations to be built with good enough accuracy (e.g. in this study, 4161 simulations were used to build the model with approximately 80% accuracy). Additionally, in operational mode, the early warning system currently presents three major weaknesses. First, due to the high-resolution of the deterministic models and thus the relative slowness of the system, the early forecast of the meteotsunami

This article is protected by copyright. All rights reserved.

hazard (at least 24-h prior to any event) is only derived once from numerical results obtained 2 days in advance. This means that the first warnings are always based on conditions forecasted from a 72-h old assimilation cycle which can lack of accuracy, particularly during extreme events. Second, human intervention is still required in the present set-up of the early warning system in order to extract the IGW parameters from the deterministic forecast. And third, to be able to provide the final meteotsunami warnings derived from hazards forecasted with input parameters extracted from the measured mean sea-level air pressures along the Italian coast and the middle Adriatic, the microbarograph data should be analyzed in a timely manner with efficient operational tools which, in the CMeEWS are still under development.

On one hand, the evaluation of the early warning system with five well-recorded events, demonstrates that (1) the IGWs driving the eastern Adriatic meteotsunamis are always forecasted and well detected, and (2) the meteotsunami hazard derived only from the deterministic model results is conservative but tends to be largely overestimated in certain locations such as Vela Luka or Vrboska. On the other hand, the evaluation in operational mode highlights the importance of (1) taking into account the uncertainties associated with the forecasted meteotsunamigenic atmospheric disturbances particularly during storm events when the deterministic model lacks of accuracy, (2) updating the final warnings using meteotsunami hazards based on input parameters extracted from the measured pressure disturbances, and (3) extending and maintaining the measurement network (microbarographs and tide gauges) along the Italian and Croatian coastlines in order to produce more accurate hazard assessments and to better understand how and where the system failed. Following these conclusions, to improve the accuracy of the warnings, for all potential future events, (1) the system should be thoroughly re-evaluated, (2) the measurements recorded by the microbarographs should be used in a timely

Author Manuscript

This article is protected by copyright. All rights reserved.

manner to derive the final hazard assessment, (3) the flooding criteria and the input parameter ranges of the surrogate model should be finely tuned as more data will become available, and (4) ultimately, once the prototype will be fully tested, the meteotsunami warnings will not only be triggered when more than 10% of the maximum elevations surpass the thresholds defined at the sensitive locations, but their strength (yellow, orange, red) will also be defined depending on the detailed statistical information (maximum, 75th-percentile, mean, median, etc.) extracted from the extreme sea-level distributions.

Finally, the CMeEWS combining 1-min air pressure measurements – accurate but scarcely spread along the Italian coast and the middle Adriatic Sea, state-of-the-art deterministic models – dedicated to meteotsunami forecast but computationally costly and slow, and a newly developed stochastic surrogate model – running at nearly zero cost but yet to be fully tested, highlights the need to use real time high-temporal resolution observational networks for regional early warning systems in the Mediterranean and presents an alternative way to deal with atmospherically-driven extreme sea-level hazard assessment.

Author Manuscript

This article is protected by copyright. All rights reserved.

Acknowledgments and data

Acknowledgement is made for the support of the ECMWF staff, in particular Xavier Abellan, as well as for ECMWF's computing and archive facilities used in this research, which has been supported by projects MESSI (UKF Grant 25/15), ADIOS (Croatian Science Foundation Grant IP-2016-06-1955) and ECMWF Special Project (The Adriatic decadal and inter-annual oscillations: modelling component). The authors would also like to thank the two anonymous reviewers for their valuable contributions. The Matlab interface developed for the stochastic surrogate model – including the gPCE coefficients needed to create the meteotsunami maximum elevation distributions at the five studied locations, as well as the WRF 1.5-km filtered results of sea surface pressure can be obtained under the Open Science Framework (OSF) FAIR data repository at https://osf.io/jysqu/ (doi:10.17605/OSF.IO/JYSQU).

Author Manuscript

This article is protected by copyright. All rights reserved.

Author Manuscript

References

Arnst, M., & Ponthot, J.-P. (2014). An overview of nonintrusive characterization, propagation, and sensitivity analysis of uncertainties in computational mechanics. Int. J. Uncertain. Quan., 4, 387–421. https://doi.org/10.1615/int.j.uncertaintyquantification.2014006990

Beven, K. J. (2006). On undermininEg the science? *Hydrological Processes*, *20*(3), 141–146.

Bulthuis, K., Arnst, M., Sun, S., & Pattyn, F. (2019). Uncertainty quantification of the multi-centennial response of the Antarctic ice sheet to climate change. *The Cryosphere*, *13*, 1349-1380. https://doi.org/10.5194/tc-13-1349-2019

Burkardt J. (2014). Slow Exponential Growth for Gauss Patterson Sparse Grids, http://people.sc.fsu.edu/~jburkardt/presentations/sgmga gps.pdf.

Cho, K.-H., Choi, J.-Y., Park K.-S., Hyun S.-K., & Park J.-Y. (2013). A synoptic study on tsunami-like sea level oscillations along the west coast of Korea using an unstructured-grid ocean model. In Conley, D. C., Masselink, G., Russell, P. E., & O'Hare, T. J. (Eds.), *Proc. 12th Int. Coastal Symposium* (Vol. 1, pp. 678–683). Plymouth, MN: Coastal Processes Research Group, School of Marine Science and Engineering, Plymouth University.

Denamiel, C., Šepić, J., & Vilibić, I. (2018). Impact of Geomorphological Changes to Harbor Resonance During Meteotsunamis: The Vela Luka Bay Test Case. *Pure Appl. Geophys.*, *175*, 3839. https://doi.org/10.1007/s00024-018-1862-5

Denamiel, C., Šepić, J., Ivanković, D., & Vilibić, I. (2019). The Adriatic Sea and Coast modelling suite: Evaluation of the meteotsunami forecast component. *Ocean Modell.*, *135*, 71–93. doi:10.1016/j.ocemod.2019.02.003

This article is protected by copyright. All rights reserved.

Author Manuscript

Dusek, G., DiVeglio, C., Licate, L., Heilman, L., Kirk, K., Paternostro, C., & Miller, A. (2019). A meteotsunami climatology along the U.S. East Coast. *Bull. Amer. Meteor. Soc.*, *0*. https://doi.org/10.1175/BAMS-D-18-0206.1

Ewing, M., Press, F., & Donn, W. L. (1954). An explanation of the Lake Michigan wave of 26 June 1954. *Science*, *120*, 684–686. doi:10.1126/science.120.3122.684

Foo, J., Yosibash, Z., & Karniadakis, G. E. (2007). Stochastic simulation of riser-sections with uncertain measured pressure loads and/or uncertain material properties. *Comput. Method. Appl. Mech. Eng.*, *196*, 4250–4271.

Formaggia, L., Guadagnini, A., Imperiali, I., Lever, V., Porta, G., Riva, M., Scotti, A. & Tamellini, L. (2013). Global sensitivity analysis through polynomial chaos expansion of a basin-scale geochemical compaction model. *Computational Geosciences*, *17*(1), 25–42. doi:10.1007/s10596-012-9311-5

Giraldi, L., Le Maître, O. P., Mandli, K. T., Dawson, C. N., Hoteit, I., & Knio, O. M. (2017). Bayesian inference of earthquake parameters from buoy data using a polynomial chaos-based surrogate. *Comput. Geosci.*, *21*(4), 683–699. https://doi.org/10.1007/s10596-017-9646-z

Ghanem, R., Higdon, R., & Owhadi, H. (2017). Handbook of Uncertainty Quantification, *Springer*. https://doi.org/10.1007/978-3-319-12385-1

Hibiya, T., & Kajiura, K. (1982). Origin of the *Abiki* phenomenon (a kind of seiche) in Nagasaki Bay. *J. Oceanogr. Soc. Jpn.*, *38*, 172–182. doi:10.1007/BF02110288

This article is protected by copyright. All rights reserved.

Knio, O. M., & Le Maître, O. P. (2006). Uncertainty propagation in CFD using polynomial chaos decomposition. *Fluid Dynamics Research*, *38*(9),616–640. doi:10.1016/j.fluiddyn.2005.12.003

Le Maître, O. P. & Knio, O. M. (2010). Spectral Methods for Uncertainty Quantification: With Applications to Computational Fluid Dynamics, *Springer Science & Business Media*. https://doi.org/10.1007/978-90-481-3520-2

Linares, A., Wu, C. H., Bechle, A. J., Anderson, E. J., & Kristovich, D. A. R. (2019). *Sci. Rep.*, *9*, 2105. doi: 10.1038/s41598-019-38716-2

Luettich, R. A., Birkhahn, R. H., & Westerink, J. J. (1991). Application of ADCIRC-2DDI to Masonboro Inlet, North Carolina: A brief numerical modeling study. Contractors Report to the US Army Engineer Waterways Experiment Station, August, 1991.

Masina, M., Archetti, R., Besio, G. & Lamberti, A. (2017). Tsunami taxonomy and detection from recent Mediterranean tide gauge data. *Coastal Engineering*, *127*, 145–169.

Monserrat, S., Vilibić, I., & Rabinovich, A. B. (2006). Meteotsunamis: atmospherically induced destructive ocean waves in the tsunami frequency band. *Nat. Hazards Earth Syst. Sci.*, *6*, 1035-1051.

Najm, H. N., Debusschere, B. J., Marzouk, Y. M., Widmer, S. & Le Maître, O. P. (2009). Uncertainty quantification in chemical systems. *Int. J. Numer. Meth. Engng.*, *80*, 789–814. doi:10.1002/nme.2551

Novak, E., Ritter, K., Schmitt, R., Steinbauer, A. (1999). Simple cubature formulas with high polynomial exactness. *Constructive Approximation*, *15*(4), 499–522.

This article is protected by copyright. All rights reserved.

Okal, E. A., Visser, J. N. J., & de Beer, C. H. (2014). The Dwarskersbos, South Africa local tsunami of August 27, 1969: field survey and simulation as a meteorological event. *Nat. Hazards, 74*, 251–268. doi:10.1007/s11069-014-1205-5

Olabarrieta, M., Valle-Levinson, A., Martinez, C. J., Pattiaratchi, C., & Shi, L. (2017). Meteotsunamis in the northeastern Gulf of Mexico and their possible link to El Niño Southern Oscillations *Nat. Hazards, 88*(3), 1325-1346. https://doi.org/10.1007/s11069-017-2922-3

Orlić, M., Belušić, D., Janeković, I., & Pasarić, M. (2010). Fresh evidence relating the great Adriatic surge of 21 June 1978 to mesoscale atmospheric forcing. *J. Geophys. Res.*, *115*, C06011. doi:10.1029/2009JC005777

Orlić, M. (2015). The first attempt at cataloguing tsunami-like waves of meteorological origin in Croatian coastal waters. *Acta Adriat.*, *56*, 83–95.

Pattiaratchi, C., & Wijeratne, E. M. S. (2014). Observations of meteorological tsunamis along the south-west Australia. *Nat. Hazards, 74*, 281–303. doi:10.1007/s11069-014-1263-8

Pellikka, H., Rauhala, J., Kahma, K. K., Tapani, S., Boman, H., & Kangas, A. (2014). Recent observations of meteotsunamis on the Finnish coast. *Nat. Hazards, 74,* 197–215. doi:10.1007/s11069-014-1150-3

Renault, L., Vizoso, G., Jansà, A., Wilkin, J., & Tintoré, J. (2011). Toward the predictability of meteotsunamis in the Balearic Sea using regional nested atmosphere and ocean models. *Geophys. Res. Lett.*, *38*, L10601. doi:10.1029/2011gl047361

Rupert, C., & Miller, C. (2007). An analysis of polynomial chaos approximations for modeling single-fluid-phase flow in porous medium systems. *J. Comput. Phys.*, *226*, 2175–2205.

This article is protected by copyright. All rights reserved.

Author Manuscript

Salaree, A., Mansouri, R., & Okal, E. A. (2018). The intriguing tsunami of 19 March 2017 at Bandar Dayyer, Iran: field survey and simulations. *Nat. Hazards*, *90*(3), 1277–1307. doi: 10.1007/s11069-017-3119-5

Šepić, J., Vilibić, I., & Strelec Mahović, N. (2012). Northern Adriatic meteorological tsunamis: observations, link to the atmosphere, and predictability. *J. Geophys. Res.*, *117*, C02002. doi:10.1029/2011JC007608

Šepić, J., Međugorac, I., Janeković, I., Dunić, N. & Vilibić, I. (2016). Multi-meteotsunami event in the Adriatic Sea generated by atmospheric disturbances of 25–26 June 2014. *Pure Appl. Geophys.*, *173*, 4117-4138. https://doi.org/10.1007/s00024-016-1249-4

Šepić, J., Vilibić, I., Beg Paklar, G., Dadić, V., Denamiel, C., Dunić, N., et al. (2017). Towards understanding and operational early warning of the Adriatic meteotsunamis: Project MESSI. *Revue Paralia*, *10*, 177–182. doi: 10.5150/cmcm.2017.033

Shchepetkin, A. F., & McWilliams, J. C. (2005). The regional oceanic modeling system: A split-explicit, free-surface, topography-following-coordinate ocean model. *Ocean Modell.*, *9*, 347–404.

Shchepetkin, A. F., & McWilliams, J. C. (2009). Correction and commentary for "Ocean forecasting in terrain-following coordinates: Formulation and skill assessment of the regional ocean modeling system" by Haidvogel et al., J. Comput. Phys., 227, pp. 3595–3624. *J. Comput. Phys.*, *228*, 8985–9000. doi:10.1016/j.jcp.2009.09.002

Sivakumar, B. (2008). Undermining the science or undermining Nature? *Hydrological Processes*, *22*, 893–897.

Author Manuscript

This article is protected by copyright. All rights reserved.

Author Manuscript

Skamarock, W. C., Klemp, J. B., Dudhia, J., Gill, D. O., Barker, D. M., Wang, W., & Powers, J. G. (2005). A Description of the Advanced Research WRF Version 2. NCAR Technical Note NCAR/TN-468+STR. doi:10.5065/D6DZ069T

Smolyak, S. A. (1963). Quadrature and interpolation formulas for tensor products of certain classes of functions. *Dokl. Akad. Nauk SSSR*, *148*(5), 1042–1045.

Soize, C., & Ghanem, R. G. (2004). Physical Systems with Random Uncertainties: Chaos Representations with Arbitrary Probability Measure. *SIAM Journal on Scientific Computing*, *26*(2), 395–410. https://doi.org/10.1137/S1064827503424505

Sraj, I., Mandli, K., Knio, O., Dawson, C. N., & Hoteit, I. (2014). Uncertainty quantification and inference of Manning's friction coefficients using DART buoy during the Tohoku tsunami. *Ocean Model.*, *83*, 82–97. doi:10.1016/j.ocemod.2014.09.001

Tanaka, K. (2010). Atmospheric pressure-wave bands around a cold front resulted in a meteo-tsunami in the East China Sea in February 2009. *Nat. Hazards Earth Syst. Sci.*, *10*, 2599–2610.

Vilibić, I., & Šepić, J. (2009). Destructive meteotsunamis along the eastern Adriatic coast: Overview. *Phys. Chem. Earth*, *34*, 904–917.

Vilibić, I., Šepić, J., Rabinovich, A.B. & Monserrat, S. (2016). Modern approaches in meteotsunami research and early warning. *Front. Mar. Sci.*, *3*(57). doi: 10.3389/fmars.2016.00057

Vučetić, T., Vilibić, I., Tinti, S., & Maramai, A. (2009). The Great Adriatic flood of 21 June 1978 revisited: An overview of the reports. *Phys. Chem. Earth*, *34*, 894–903.

This article is protected by copyright. All rights reserved.

Wang, M., Wan, Z., & Huang, Q. (2016). A New Uncertain Analysis Method for the Prediction of Acoustic Field with Random and Interval Parameters. *Shock and Vibration*, 16 pp. https://doi.org/10.1155/2016/3693262

Warner, J. C., Armstrong, B., He, R., & Zambon, J. B. (2010). Development of a Coupled Ocean-Atmosphere-Wave-Sediment Transport (COAWST) modeling system. *Ocean Modell.*, 35, 230-244.

Whitmore, P., & White, B. (2014). Meteotsunami forecasting: sensitivities demonstrated by the 2008 Boothbay, Maine, event. *Nat. Hazards*, *74*, 11–24. doi:10.1007/s11069-014-1056-0

Xiu, D., & Karniadakis, G. E. (2002). The Wiener--Askey Polynomial Chaos for Stochastic Differential Equations. *SIAM Journal on Scientific Computing*, *24*(2), 619–644. https://doi.org/10.1137/S1064827501387826

Author Manuscript

This article is protected by copyright. All rights reserved.

Figure 1.

Author Manuscript

This article is protected by copyright. All rights reserved.

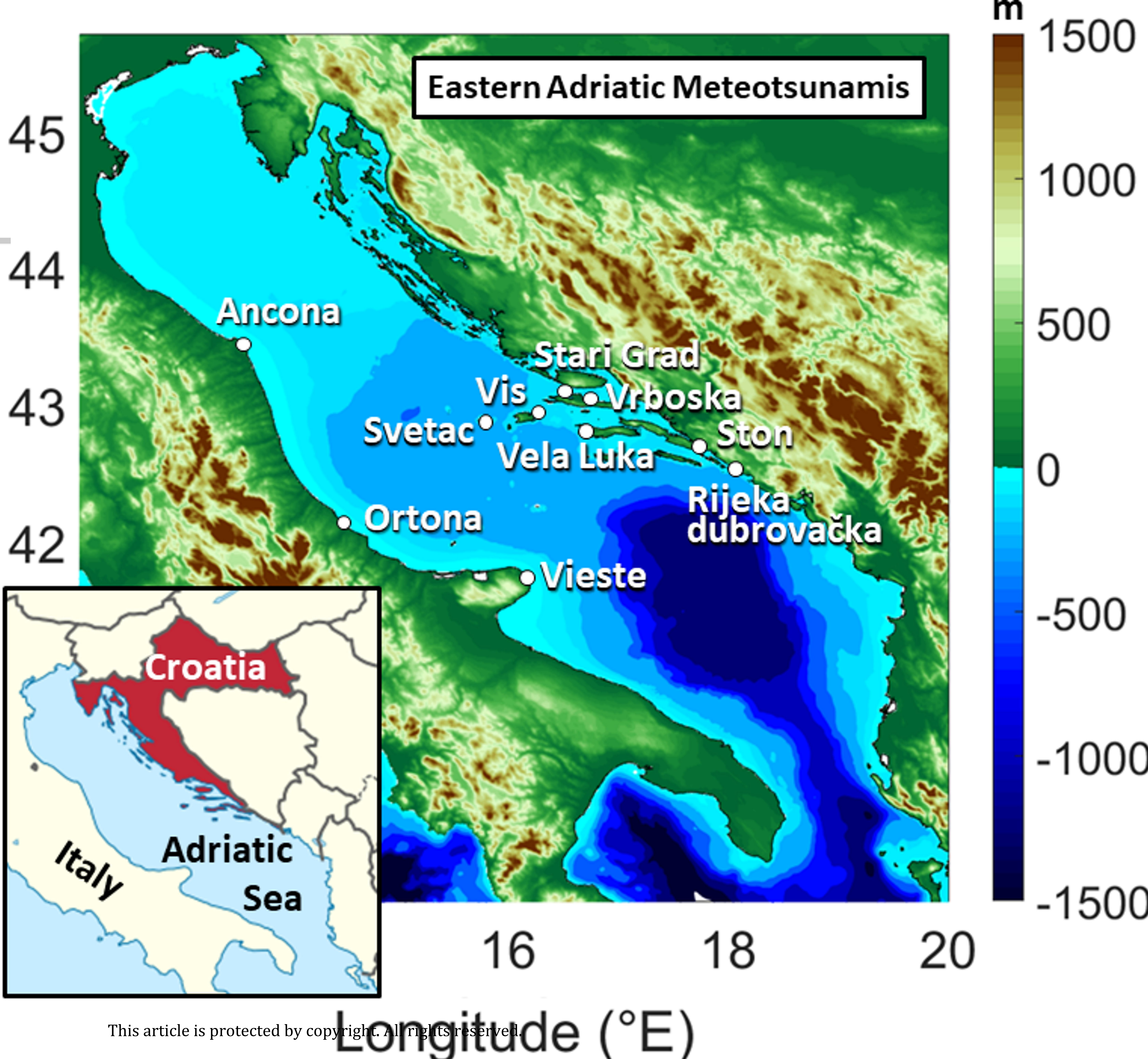

Author Manuscript

This article is protected by copyright. All rights reserved.

Figure 2.

Author Manuscript

This article is protected by copyright. All rights reserved.

Author Manuscript

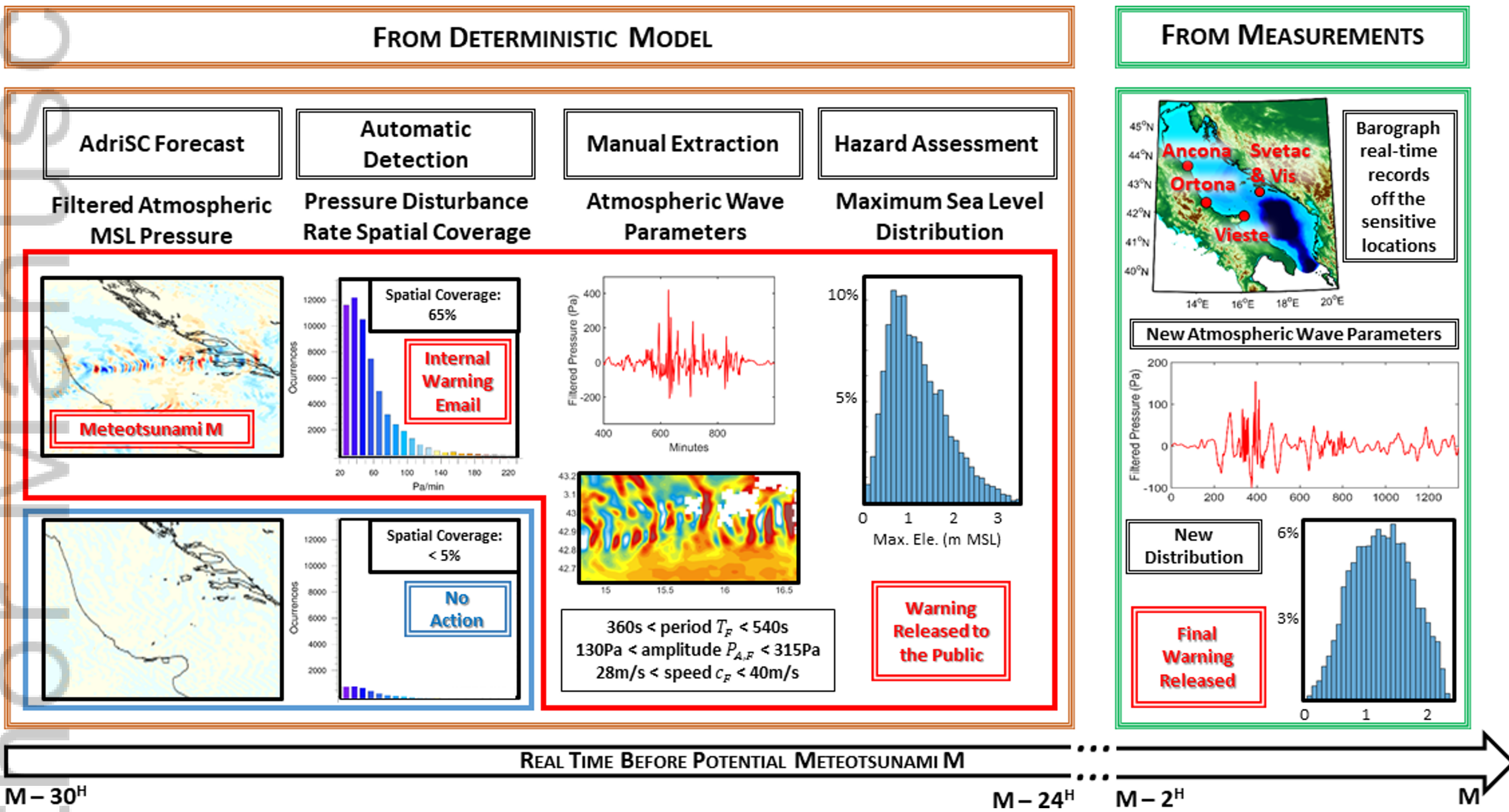

This article is protected by copyright. All rights reserved.

Figure 3.

Author Manuscript

This article is protected by copyright. All rights reserved.

Author Manuscript

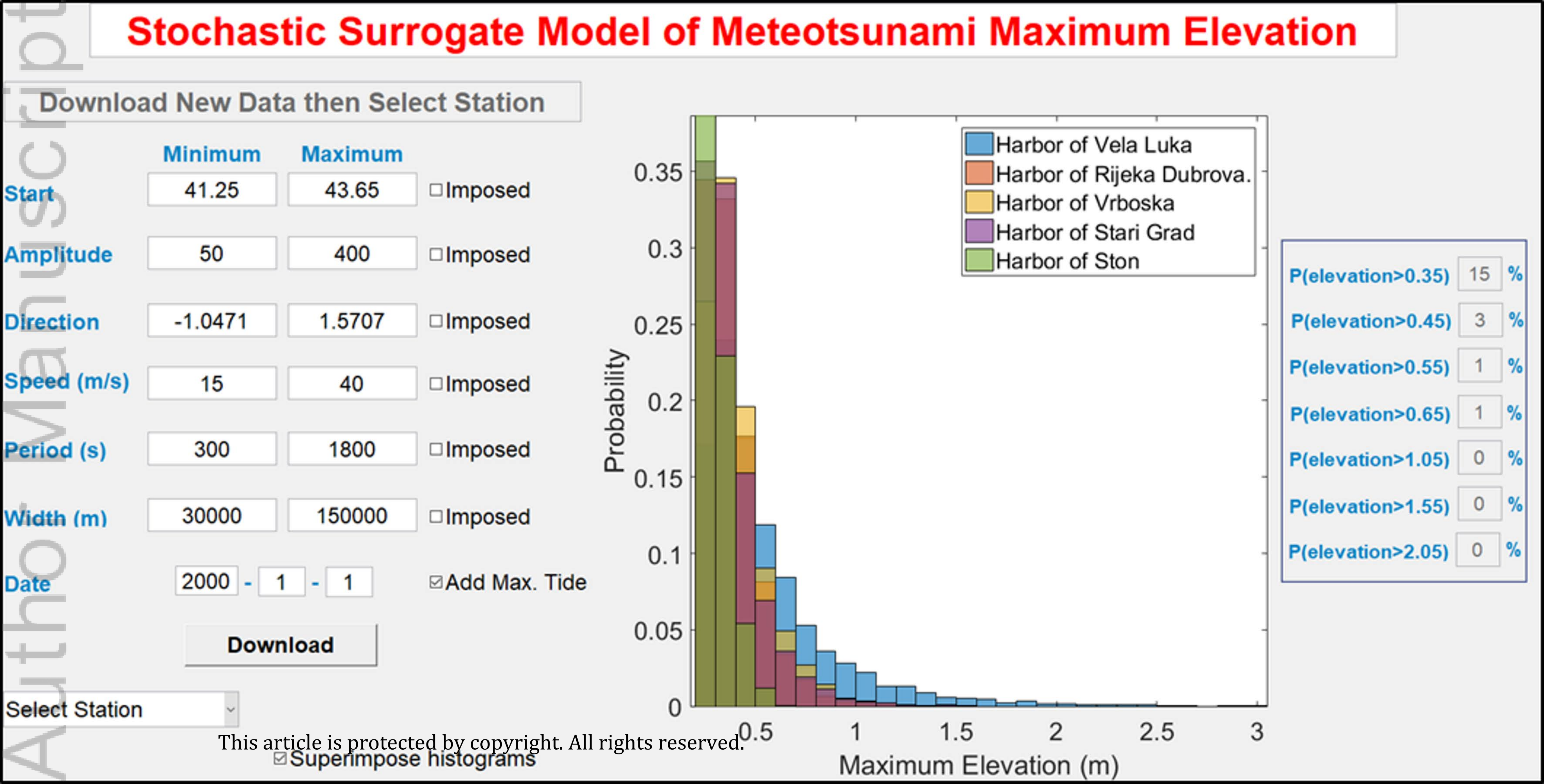

This article is protected by copyright. All rights reserved.

Figure 4.

Author Manuscript

This article is protected by copyright. All rights reserved.

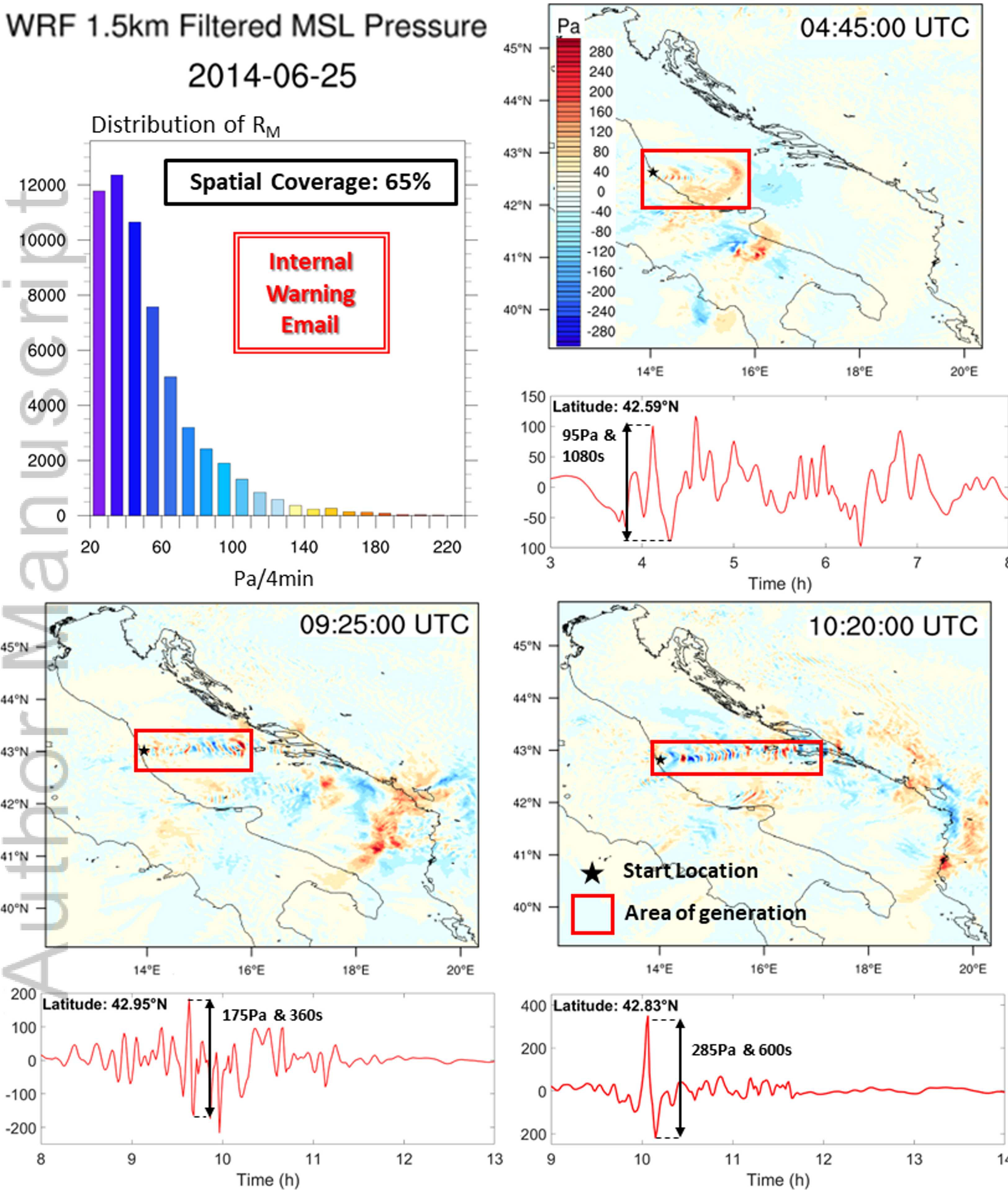

This article is protected by copyright. All rights reserved.

Figure 5.

Author Manuscript

This article is protected by copyright. All rights reserved.

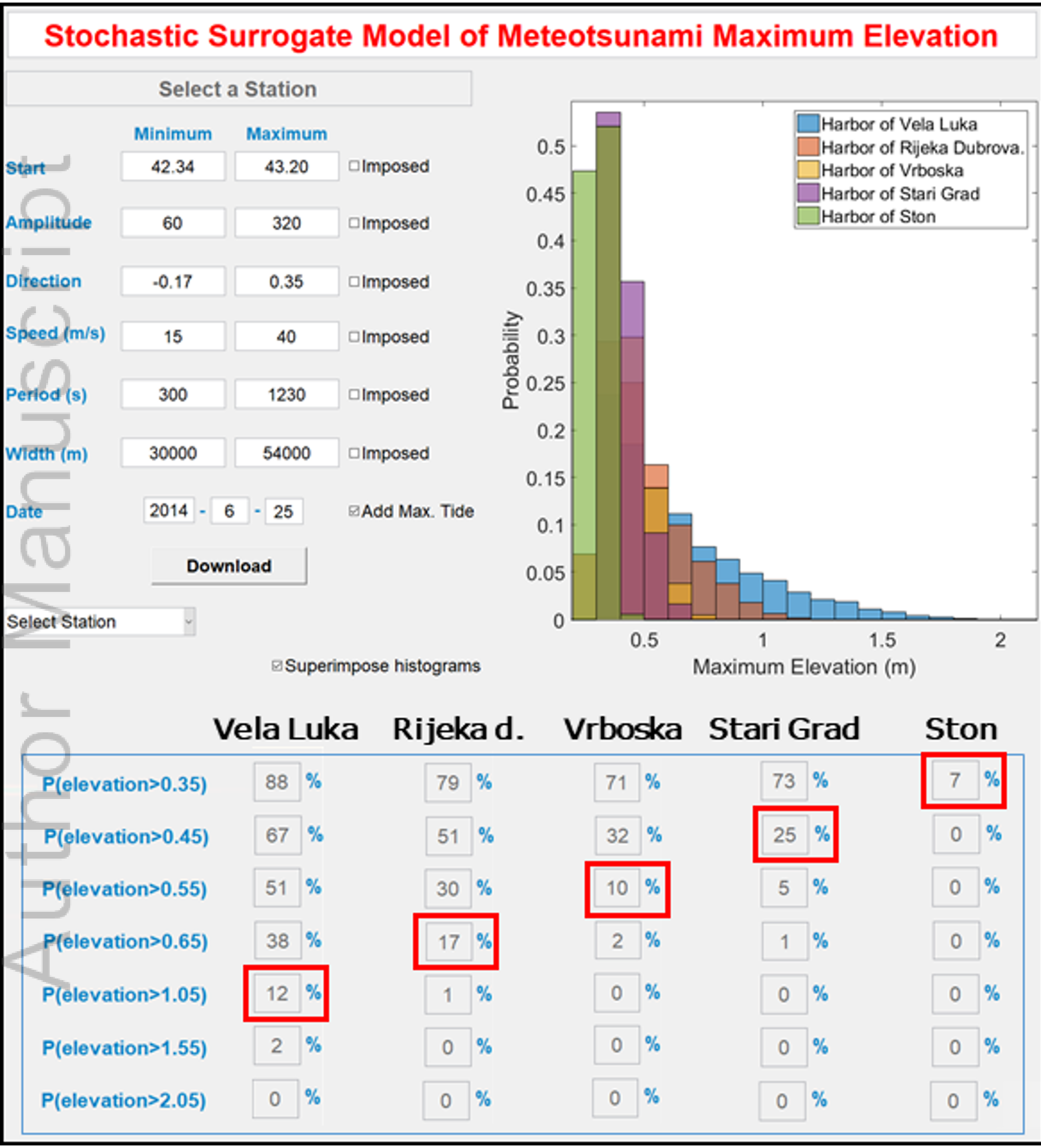

Author Manuscript

This article is protected by copyright. All rights reserved.

Figure 6.

Author Manuscript

This article is protected by copyright. All rights reserved.

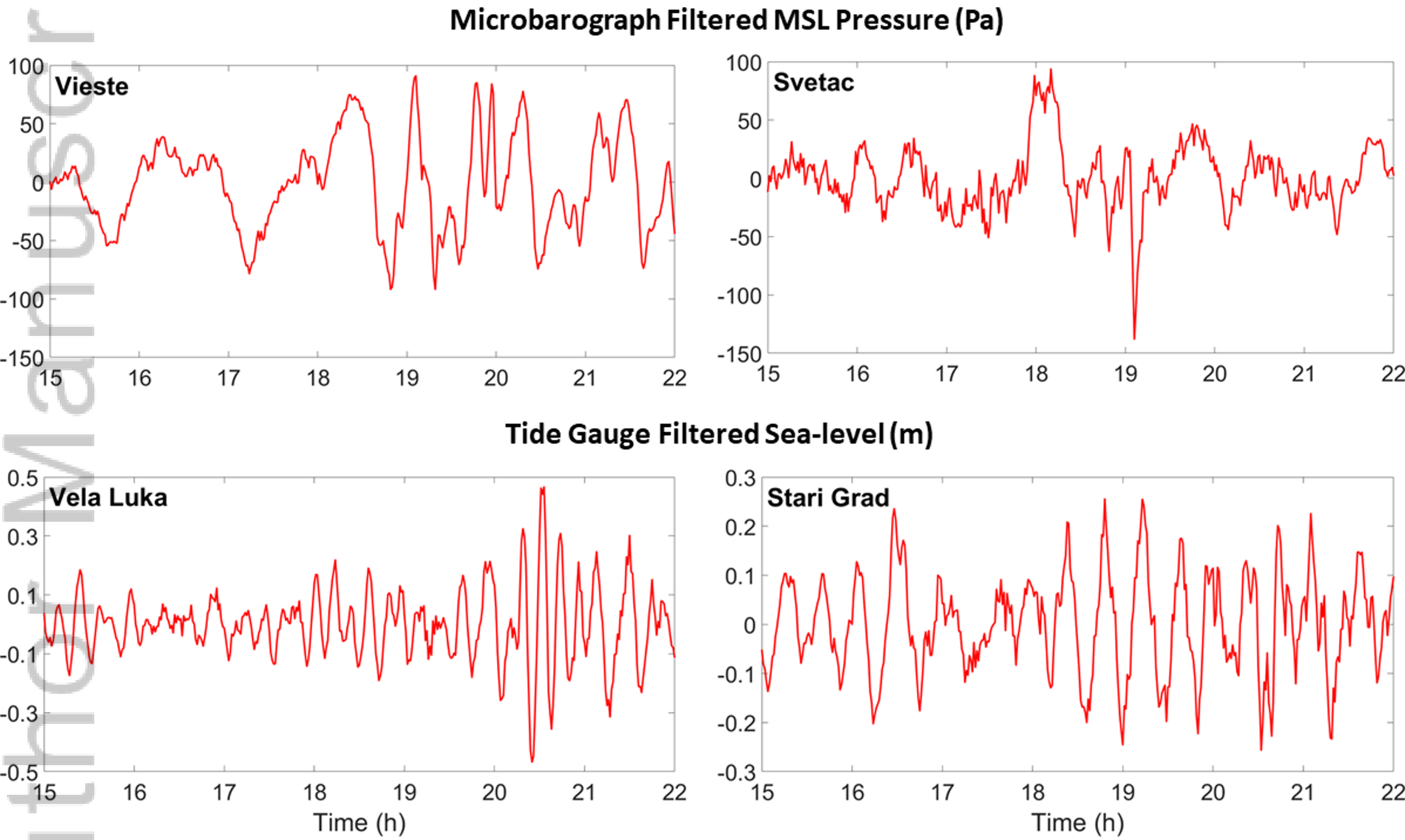

Author Manuscript

This article is protected by copyright. All rights reserved.

Figure 7.

Author Manuscript

This article is protected by copyright. All rights reserved.

Author Manuscript

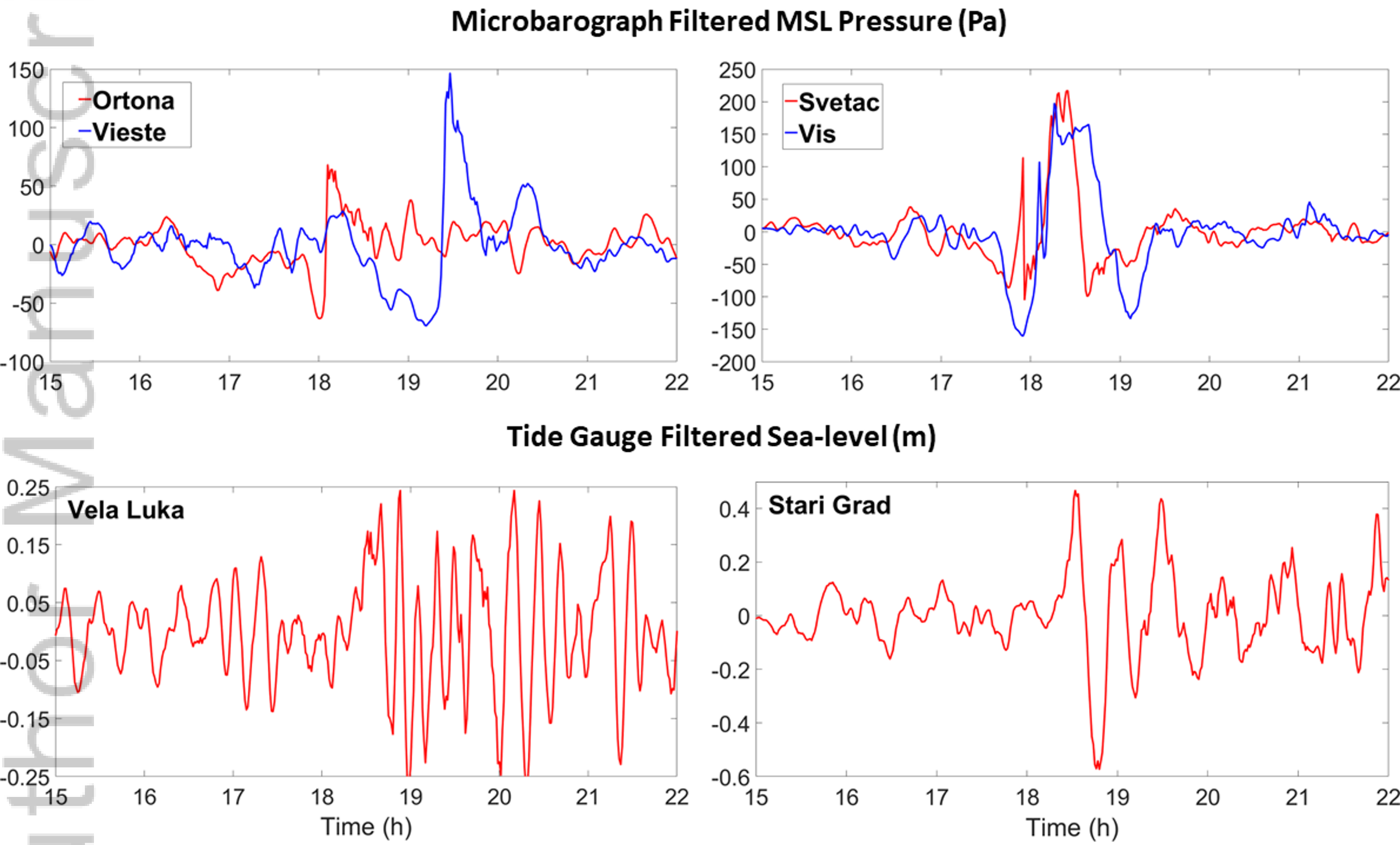

This article is protected by copyright. All rights reserved.

Figure 8.

Author Manuscript

This article is protected by copyright. All rights reserved.

Author Manuscript

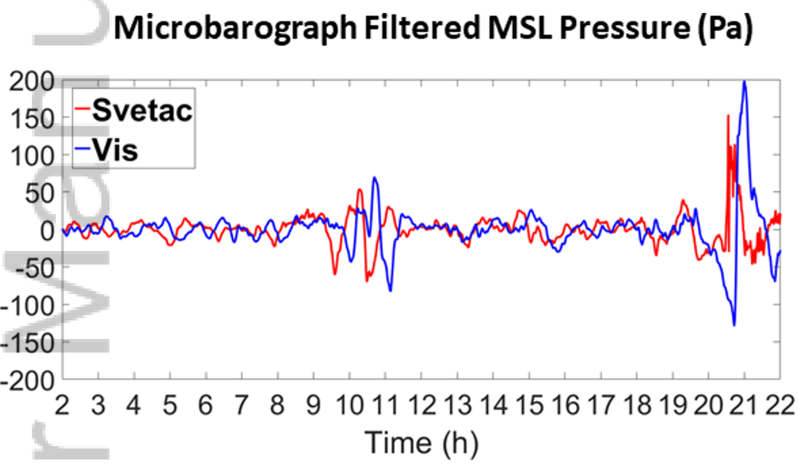

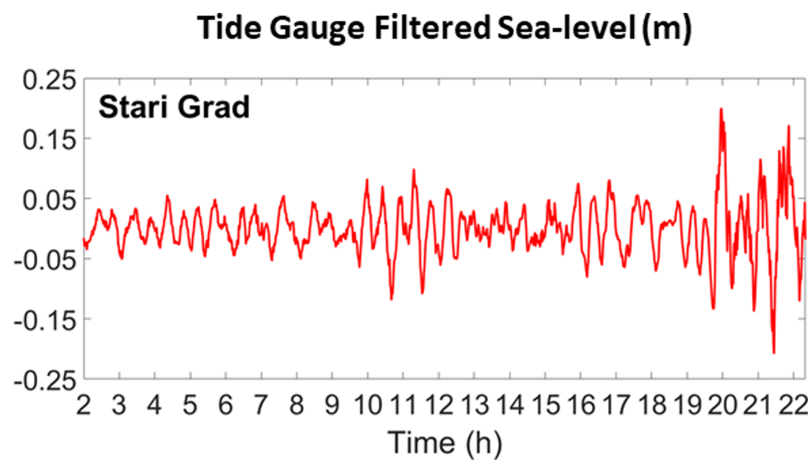

This article is protected by copyright. All rights reserved.

Author Manuscript

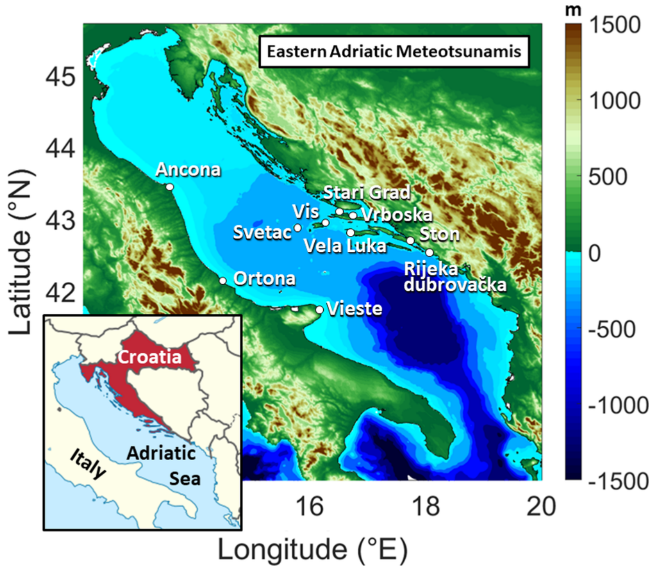

2019JC015574-f01-z-.tif

This article is protected by copyright. All rights reserved.

Author Manuscript

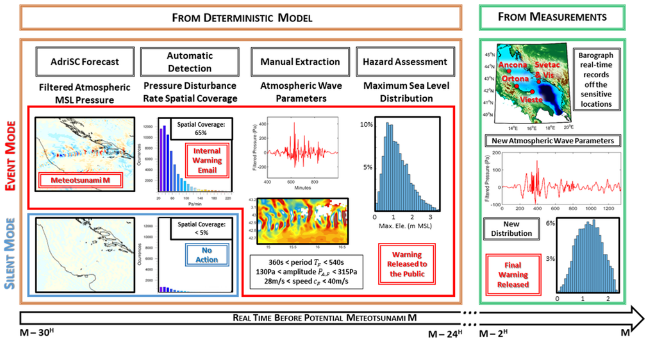

2019JC015574-f02-z-.tif

This article is protected by copyright. All rights reserved.

Author Manuscript

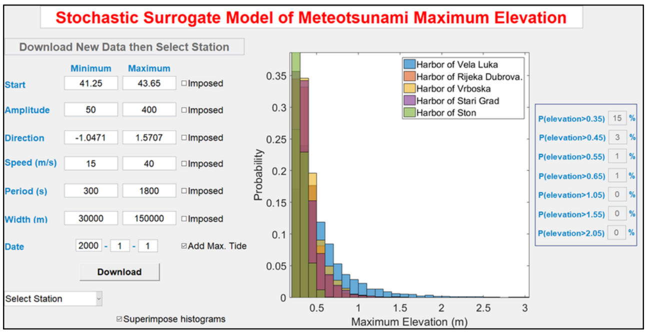

2019JC015574-f03-z-.tif

This article is protected by copyright. All rights reserved.

Author Manuscript

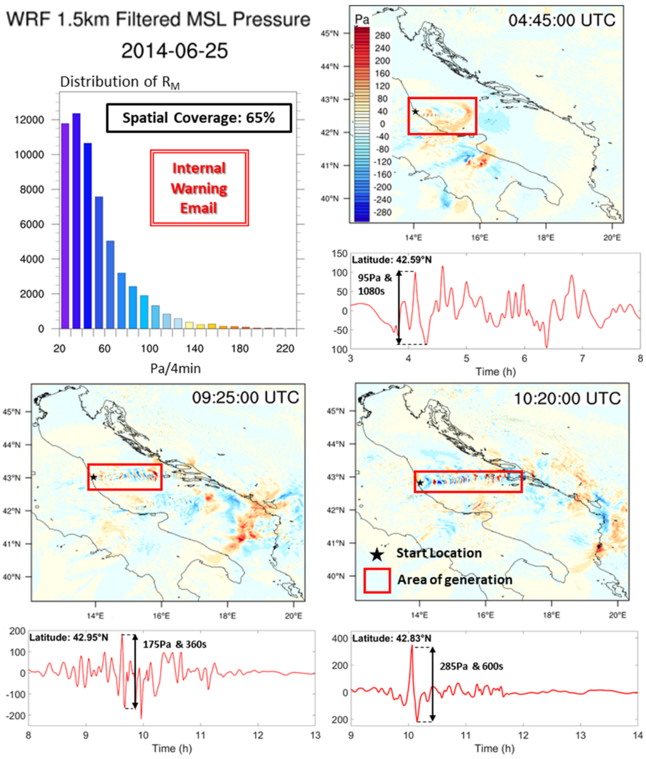

2019JC015574-f04-z-.tif

This article is protected by copyright. All rights reserved.

Author Manuscript

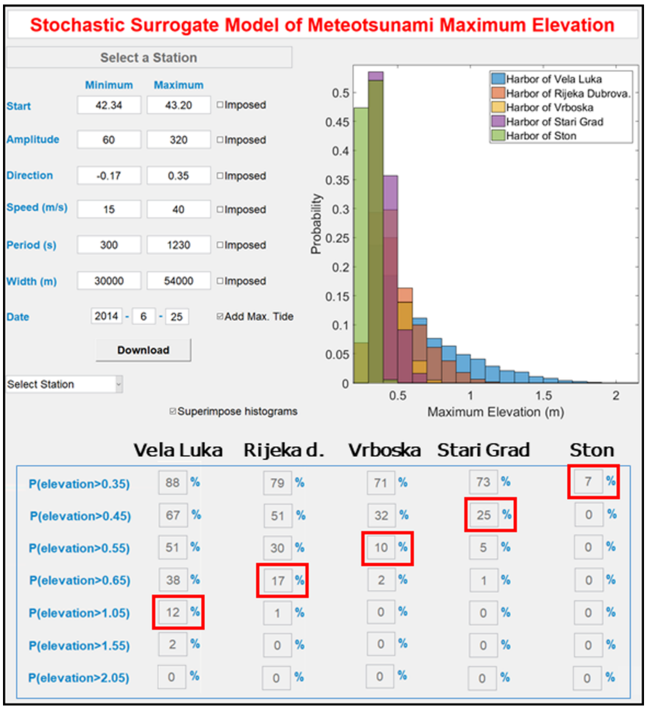

2019JC015574-f05-z-.tif

This article is protected by copyright. All rights reserved.

Author Manuscript

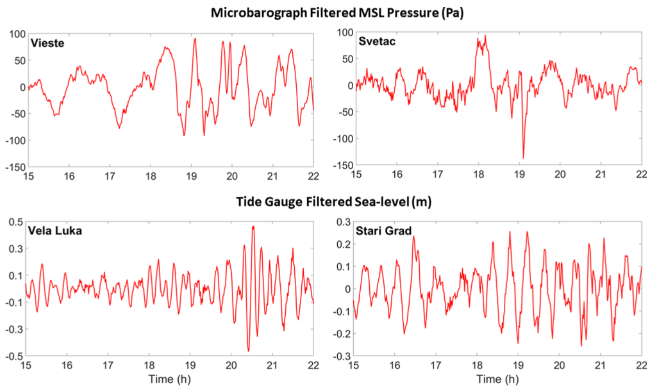

2019JC015574-f06-z-.tif

This article is protected by copyright. All rights reserved.

Author Manuscript

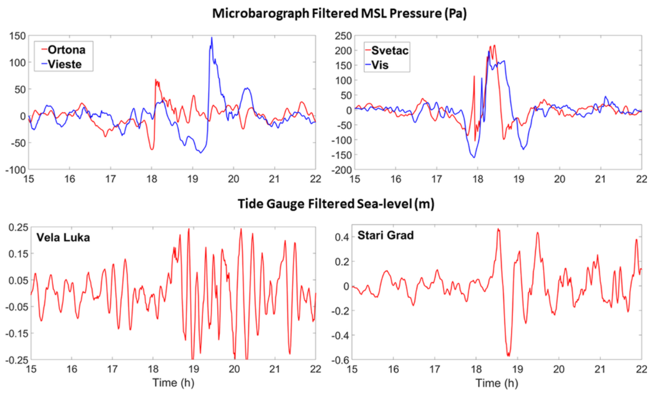

2019JC015574-f07-z-.tif

This article is protected by copyright. All rights reserved.

Author Manuscript

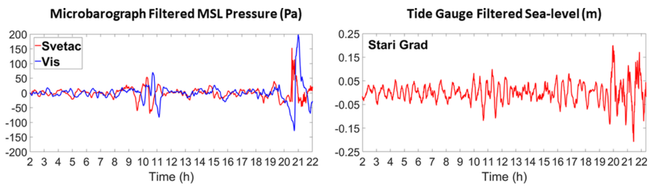

2019JC015574-f08-z-.tif

This article is protected by copyright. All rights reserved.